5 Low-energy constants

Authors: S. Dürr, H. Fukaya, U. M. Heller

5.1 Chiral perturbation theory and lattice QCD

In the study of the quark-mass dependence of QCD observables calculated on the lattice, it is beneficial to use chiral perturbation theory (χPT). This framework predicts the nonanalytic quark-mass dependence of hadron masses and matrix elements, and it provides symmetry relations among such observables. These predictions invoke a set of linearly independent and universal (i.e., process-independent) low-energy constants (LECs), defined as coefficients of the polynomial terms (in m_q or M_π^2) of different observables.

χPT is an effective field theory approach to the low-energy properties of QCD based on the spontaneous breaking of chiral symmetry, $SU(N_f)_L \times SU(N_f)_R \to SU(N_f)_V$, and its soft explicit breaking by quark-mass terms. In its original implementation (i.e., in infinite volume) it is an expansion in powers of m_q and p^2 with the counting rule $M_\pi^2 \sim m_q \sim p^2$.

If one expands around the $SU(2)$ chiral limit, two LECs appear at order p^2 in the chiral effective Lagrangian,

$$F \equiv F_\pi \Big|_{m_u, m_d \to 0} \qquad \text{and} \qquad B \equiv \frac{\Sigma}{F^2}, \quad \text{where} \quad \Sigma \equiv -\langle \bar{u}u \rangle \Big|_{m_u, m_d \to 0}, \qquad (87)$$

and seven more at order p^4, called $\bar{\ell}_i$ with $i = 1, \ldots, 7$. In the analysis of the $SU(3)$ chiral limit there are again[1] two LECs at order p^2,

$$F_0 \equiv F_\pi \Big|_{m_u, m_d, m_s \to 0} \qquad \text{and} \qquad B_0 \equiv \frac{\Sigma_0}{F_0^2}, \quad \text{where} \quad \Sigma_0 \equiv -\langle \bar{u}u \rangle \Big|_{m_u, m_d, m_s \to 0}, \qquad (88)$$

but ten more at order p^4, indicated by the symbols $L_i(\mu)$ with $i = 1, \ldots, 10$. These "constants" are independent of the quark masses[2], but they become scale dependent after renormalization (sometimes a superscript r is used). The $SU(2)$ constants $\bar{\ell}_i$ are μ-independent, since they are defined at scale $\mu = M_\pi^{\text{phys}}$ (as indicated by the bar). The $SU(3)$ constants $L_i(\mu)$ are usually quoted at the renormalization scale $\mu = 770\,\text{MeV}$. For the precise definition of these constants and their scale dependence we refer the reader to Refs. [1, 2].

In the previous four versions of the FLAG review, we summarized the χPT formulae for the quark-mass dependence of the pion and kaon mass and decay constant, as well as the scalar and vector pion charge radius. We briefly discussed the different regimes of χPT, touched on partially quenched and mixed action formulations, collected and colour-coded the available lattice results for the LECs considered, and formed FLAG estimates or averages, where possible.

---

[1]Here and in the following, we stick to the notation used in the papers where the χPT formulae were established, i.e., we work with $F_\pi \equiv f_\pi/\sqrt{2} = 92.2(1)\,\text{MeV}$ and $F_K \equiv f_K/\sqrt{2}$. The occurrence of different normalization conventions is not convenient, but avoiding it by reformulating the formulae in terms of f_π, f_K is not a good way out. Since we are using different symbols, confusion cannot arise.

[2]More precisely, they are independent of the 2 or 3 light-quark masses that are explicitly considered in the respective framework. However, all low-energy constants depend on the masses of the remaining quarks s, c, b, t or c, b, t in the $SU(2)$ and $SU(3)$ framework, respectively, although the dependence on the masses of the c, b, t quarks is expected to be small [1, 2].

Since the fourth edition in 2019 [3] (referred to as FLAG 19 below) only a handful of papers appeared with results on the set of LECs covered in our report, but none that qualifies to be included in an average. We therefore decided to shorten the section on LECs considerably, referring the reader to the 2019 FLAG review for the χPT formulae, description of the results covered there, and the details and explanation of the FLAG estimates and averages. In this edition, we will concentrate on the description of the new results and, for the convenience of our readers, list the FLAG estimates and averages, asking the reader to consult FLAG 19 [3] for the details.

In the 2019 edition, we introduced a section on $\pi\pi$ scattering in the context of $SU(2)$ χPT and collected results, from finite-volume lattice calculations, of the isospin $I = 0$ and $I = 2$ scattering lengths. In this edition, we will keep this section and describe the new results that appeared since the 2019 FLAG review. We will, further, add a section on πK and KK scattering in the context of $SU(3)$ χPT and collect the available results for the scattering lengths from finite-volume lattice calculations.

5.1.1 $\pi\pi$ scattering

The scattering of pseudoscalar octet mesons off each other (mostly $\pi\pi$ and πK scattering) is a useful approach to determine χPT low-energy constants [4–8]. This statement holds true both in experiment and on the lattice. We would like to point out the main difference between these two approaches is not so much the discretization of space-time, but rather the Minkowskian versus Euclidean setup.

In infinite-volume Minkowski space-time, 4-point Green's functions can be evaluated (e.g., in experiment) for a continuous range of (on-shell) momenta, as captured, for instance, by the Mandelstam variable s. For a given isospin channel $I = 0$ or $I = 2$ the $\pi\pi$ scattering phase shift $\delta^I(s)$ can be determined for a variety of s values, and by matching to χPT some low-energy constants can be determined (see below). In infinite-volume Euclidean space-time, such 4-point Green's functions can only be evaluated at kinematic thresholds; this is the content of the so-called Maiani-Testa theorem [9]. However, in the Euclidean case, the finite volume comes to our rescue, as first pointed out by Lüscher [10–13]. By comparing the energy of the (interacting) two-pion system in a box with finite spatial extent L to twice the energy of a pion (with identical bare parameters) in infinite volume information on the scattering length can be obtained. In particular, in the (somewhat idealized) situation where one can "scan" through a narrowly spaced set of box-sizes L such information can be reconstructed in an efficient way.

We begin with a brief summary of the relevant formulae in $SU(2)$ χPT terminology. In the x-expansion the formulae for a_ℓ^I with $\ell = 0$ and $I = 0, 2$ are found in Ref. [1]

$$a_0^0 M_\pi \;=\; +\frac{7M^2}{32\pi F^2}\left\{1 + \frac{5M^2}{84\pi^2 F^2}\left[\bar{\ell}_1 + 2\bar{\ell}_2 - \frac{9}{10}\bar{\ell}_3 + \frac{21}{8}\right] + \mathcal{O}(x^2)\right\}, \qquad (89)$$

$$a_0^2 M_\pi \;=\; -\frac{M^2}{16\pi F^2}\left\{1 - \frac{M^2}{12\pi^2 F^2}\left[\bar{\ell}_1 + 2\bar{\ell}_2 + \frac{3}{8}\right] + \mathcal{O}(x^2)\right\}, \qquad (90)$$

where $x \equiv M^2/(4\pi F)^2$ with $M^2 = (m_u + m_d)\Sigma/F^2$ is one possible expansion parameter of χPT. Throughout this report we deviate from the χPT habit of absorbing a factor $-M_\pi$ into the scattering length (relative to the convention used in quantum mechanics); we include just a minus sign but not the factor M_π. Hence, our a_ℓ^I have the dimension of a length so that all

quark- or pion-mass dependence is explicit (as is most convenient for the lattice community). But the sign convention is the one of the chiral community (where $a_\ell^I M_\pi > 0$ means attraction and $a_\ell^I M_\pi < 0$ indicates repulsion).

An important difference between the two S-wave scattering lengths is evident already at tree-level. The isospin-0 scattering length (89) is large and positive at this order, while the isospin-2 counterpart (90) is by a factor ~ 3.5 smaller (in absolute magnitude) and negative. Hence, in the channel with $I = 0$ the interaction is *attractive*, while in the channel with $I = 2$ the interaction is *repulsive* and significantly weaker. In this convention, experimental results, evaluated with the unitarity constraint germane to any local quantum field theory, read $a_0^0 M_\pi = 0.2198(46)_{\text{stat}}(16)_{\text{syst}}(64)_{\text{theo}}$ and $a_0^2 M_\pi = -0.0445(11)_{\text{stat}}(4)_{\text{syst}}(8)_{\text{theo}}$ [7, 14–16]. The ratio between the two (absolute) central values is about 4.9, i.e., a bit larger than 3.5. This, in turn, suggests that NLO contributions to a_0^0 and a_0^2 are sizeable, but the expansion seems well behaved.

Equations (89, 90) may be recast in the ξ-expansion, with $\xi \equiv M_\pi^2/(4\pi F_\pi)^2$, as

$$a_0^0 M_\pi = +\frac{7M_\pi^2}{32\pi F_\pi^2}\left\{1 + \xi\frac{1}{2}\bar{\ell}_3 + \xi 2\bar{\ell}_4 + \xi\left[\frac{20}{21}\bar{\ell}_1 + \frac{40}{21}\bar{\ell}_2 - \frac{18}{21}\bar{\ell}_3 + \frac{5}{2}\right] + \mathcal{O}(\xi^2)\right\}, \quad (91)$$

$$a_0^2 M_\pi = -\frac{M_\pi^2}{16\pi F_\pi^2}\left\{1 + \xi\frac{1}{2}\bar{\ell}_3 + \xi 2\bar{\ell}_4 - \xi\left[\frac{4}{3}\bar{\ell}_1 + \frac{8}{3}\bar{\ell}_2 + \frac{1}{2}\right] + \mathcal{O}(\xi^2)\right\}, \quad (92)$$

where $M^2/(4\pi F)^2 = M_\pi^2/(4\pi F_\pi)^2\{1 + \frac{1}{2}\xi\bar{\ell}_3 + 2\xi\bar{\ell}_4 + \mathcal{O}(\xi^2)\}$ has been used. Finally, this expression can be summarized as

$$a_0^0 M_\pi = +\frac{7M_\pi^2}{32\pi F_\pi^2}\left\{1 + \frac{9M_\pi^2}{32\pi^2 F_\pi^2}\ln\frac{(\lambda_0^0)^2}{M_\pi^2} + \mathcal{O}(\xi^2)\right\}, \quad (93)$$

$$a_0^2 M_\pi = -\frac{M_\pi^2}{16\pi F_\pi^2}\left\{1 - \frac{3M_\pi^2}{32\pi^2 F_\pi^2}\ln\frac{(\lambda_0^2)^2}{M_\pi^2} + \mathcal{O}(\xi^2)\right\}, \quad (94)$$

with the abbreviations

$$\frac{9}{2}\ln\frac{(\lambda_0^0)^2}{M_{\pi,\text{phys}}^2} = \frac{20}{21}\bar{\ell}_1 + \frac{40}{21}\bar{\ell}_2 - \frac{5}{14}\bar{\ell}_3 + 2\bar{\ell}_4 + \frac{5}{2}, \quad (95)$$

$$\frac{3}{2}\ln\frac{(\lambda_0^2)^2}{M_{\pi,\text{phys}}^2} = \frac{4}{3}\bar{\ell}_1 + \frac{8}{3}\bar{\ell}_2 - \frac{1}{2}\bar{\ell}_3 - 2\bar{\ell}_4 + \frac{1}{2}, \quad (96)$$

where λ_ℓ^I with $\ell = 0$ and $I = 0, 2$ are scales like the Λ_i in $\bar{\ell}_i = \ln(\Lambda_i^2/M_{\pi,\text{phys}}^2)$ for $i \in \{1, 2, 3, 4\}$ (albeit they are not independent from the latter). Here, we made use of the fact that $M_\pi^2/M_{\pi,\text{phys}}^2 = 1 + \mathcal{O}(\xi)$ and thus $\xi\ln(M_\pi^2/M_{\pi,\text{phys}}^2) = \mathcal{O}(\xi^2)$. In the absence of any knowledge on the $\bar{\ell}_i$, one would assume $\lambda_0^0 \simeq \lambda_0^2$, and with this input Eqs. (93, 94) suggest that the NLO contribution to $|a_0^0|$ is by a factor ~ 10.5 larger than the NLO contribution to $|a_0^2|$. The experimental numbers quoted before clearly support this view.

Given that all of this sounds like a complete success story for the determination of the scattering lengths a_0^0 and a_0^2, one may wonder whether lattice QCD is helpful at all. It is, because the "experimental" evaluation of these scattering lengths builds on a constraint between these two quantities that, in turn, is based on a (rather nontrivial) dispersive evaluation of scattering phase shifts [7, 14–16]. Hence, to overcome this possible loophole, an independent lattice determination of a_0^0 and/or a_0^2 is highly welcome.

On the lattice a_0^2 is much easier to determine than a_0^0, since the former quantity does not involve quark-line disconnected contributions. The main upshot (to be reviewed below) is that the lattice determination of $a_0^2 M_\pi$ at the physical mass point is in perfect agreement with the experimental numbers quoted before, thus supporting the view that the scalar condensate is—at least in the $SU(2)$ case—the dominant order parameter, and the original estimate $\bar{\ell}_3 = 2.9 \pm 2.4$ is correct (see below). Still, from a lattice perspective it is natural to see a determination of $a_0^0 M_\pi$ and/or $a_0^2 M_\pi$ as a means to access the specific linear combinations of $\bar{\ell}_i$ with $i \in \{1, 2, 3, 4\}$ defined in Eqs. (95, 96).

In passing, we note that an alternative version of Eqs. (93, 94) is used in the literature, too. For instance, Refs. [17–21] give their results in the form

$$a_0^0 M_\pi \;\; = \;\; +\frac{7M_\pi^2}{32\pi F_\pi^2}\left\{1 + \frac{M_\pi^2}{32\pi^2 F_\pi^2}\left[\ell_{\pi\pi}^{I=0} + 5 - 9\ln\frac{M_\pi^2}{2F_\pi^2}\right] + \mathcal{O}(\xi^2)\right\} , \tag{97}$$

$$a_0^2 M_\pi \;\; = \;\; -\frac{M_\pi^2}{16\pi F_\pi^2}\left\{1 - \frac{M_\pi^2}{32\pi^2 F_\pi^2}\left[\ell_{\pi\pi}^{I=2} + 1 - 3\ln\frac{M_\pi^2}{2F_\pi^2}\right] + \mathcal{O}(\xi^2)\right\} , \tag{98}$$

where the quantities (used to quote the results of the lattice calculation)

$$\ell_{\pi\pi}^{I=0} \;\; = \;\; \frac{40}{21}\bar{\ell}_1 + \frac{80}{21}\bar{\ell}_2 - \frac{5}{7}\bar{\ell}_3 + 4\bar{\ell}_4 + 9\ln\frac{M_{\pi,\text{phys}}^2}{2F_{\pi,\text{phys}}^2} , \tag{99}$$

$$\ell_{\pi\pi}^{I=2} \;\; = \;\; \frac{8}{3}\bar{\ell}_1 + \frac{16}{3}\bar{\ell}_2 - \bar{\ell}_3 - 4\bar{\ell}_4 + 3\ln\frac{M_{\pi,\text{phys}}^2}{2F_{\pi,\text{phys}}^2} , \tag{100}$$

amount to linear combinations of the $\ell_i^{\text{ren}}(\mu^{\text{ren}})$ that, due to the explicit logarithms in Eqs. (99, 100), are effectively renormalized at the scale $\mu_{\text{ren}} = f_\pi^{\text{phys}} = \sqrt{2}F_\pi^{\text{phys}} = 130.41(20)\,\text{MeV}$ [22]. Note that in these equations the dependence on the *physical* pion mass in the logarithms cancels the one that comes from the $\bar{\ell}_i$, so that the right-hand-sides bear no knowledge of M_π^{phys}. This alternative form is slightly different from Eqs. (93, 94). Exact equality would be reached upon substituting $F_\pi^2 \to F_{\pi,\text{phys}}^2$ in the logarithms of Eqs. (97, 98). Upon expanding $F_\pi^2/F_{\pi,\text{phys}}^2$ and subsequently the logarithm, one realizes that this difference amounts to a term $\mathcal{O}(\xi)$ within the square bracket. It thus makes up for a difference at the NNLO, which is beyond the scope of these formulae.

We close by mentioning a few works that elaborate on specific issues in $\pi\pi$ scattering relevant to the lattice. Reference [23] does mixed action χPT for 2 and 2+1 flavours of staggered sea quarks and Ginsparg-Wilson valence quarks, Refs. [24, 25] work out scattering formulae in Wilson fermion χPT, and Ref. [26] lists connected and disconnected contractions in $\pi\pi$ scattering.

5.1.2 πK and KK scattering

The discussion of $\pi\pi$ scattering in the previous subsection carries over, without material changes, to the case of πK and KK scattering. The one (tiny) difference is that results, if contact with χPT is desired, must be matched against the $SU(3)$ version of this framework. In other words, for $\pi\pi$ scattering there is a choice between $SU(2)$ and $SU(3)$, while for πK and KK scattering matching to the $SU(3)$ version of χPT is mandatory[3].

---

[3]Note that this could be circumvented if one used a heavy-meson extended version of χPT, in particular $SU(2)$ χPT with an extra (heavy) strange quark [27–29]. However, we have the original Gasser-Leutwyler versions of $SU(2)$ and $SU(3)$ χPT in mind.

For completeness we also include, below, the $SU(3)$ χPT result for $I = 2$ $\pi\pi$ scattering. Since, as in the FLAG 19 review, we tabulate the S-wave scattering length with combined isospin I in the dimensionless variable $a_0^I M_\pi$, where the physical pion mass is meant, the result can be converted into specific linear combinations of NLO χPT coefficients in either the $SU(2)$ or $SU(3)$ χPT framework. In this conversion, an extra piece to the systematic error is to be included, to account for higher-order terms in the chiral expansion.

Below, we continue this tradition by summarizing results in the dimensionless variable $a_0^I \mu_{\pi K}$ for πK scattering and $a_0^I M_K$ for KK scattering. Throughout this report, $\mu_{\pi K} \equiv M_\pi M_K / (M_\pi + M_K)$ is the reduced mass of the kaon-pion system at the physical mass point. Again, these results can be converted into linear combinations of the L_i, with proper adjustment of the systematic uncertainty, due to the chiral expansion. In doing so, one should keep in mind that the $SU(3)$ framework does not converge as swiftly as the $SU(2)$ frameork, since $m_{ud} \ll m_s$.

We basically follow Ref. [30], but we adopt, for masses and decay constants, the conventions of the LEC section in the FLAG 19 report. We consider the χPT formulae at $\mathcal{O}(p^4)$ in the chiral expansion, as given in Refs. [2, 31–35]. The scattering lengths of the $\pi\pi(I = 2)$, $KK(I = 1)$, $\pi K(I = \frac{3}{2})$ and $\pi K(I = \frac{1}{2})$ systems can be written as

$$a_{0,\pi\pi}^2 M_\pi = \frac{M_\pi^2}{16\pi F_\pi^2}\left\{ -1 + \frac{16}{F_\pi^2}\left[M_\pi^2 L_{\text{scat}}(\mu) - \frac{M_\pi^2}{2}L_5(\mu) + \chi_{\pi\pi}^2(\mu) \right] \right\}, \tag{101}$$

$$a_{0,KK}^1 M_K = \frac{M_K^2}{16\pi F_K^2}\left\{ -1 + \frac{16}{F_K^2}\left[M_K^2 L_{\text{scat}}(\mu) - \frac{M_K^2}{2}L_5(\mu) + \chi_{KK}^1(\mu) \right] \right\}, \tag{102}$$

$$a_{0,\pi K}^{3/2} \mu_{\pi K} = \frac{\mu_{\pi K}^2}{8\pi F_\pi F_K}\left\{ -1 + \frac{16}{F_\pi F_K}\left[M_\pi M_K L_{\text{scat}}(\mu) - \frac{M_\pi^2 + M_K^2}{4}L_5(\mu) + \chi_{\pi K}^{3/2}(\mu) \right] \right\} \tag{103}$$

$$a_{0,\pi K}^{1/2} \mu_{\pi K} = \frac{\mu_{\pi K}^2}{8\pi F_\pi F_K}\left\{ 2 + \frac{16}{F_\pi F_K}\left[M_\pi M_K L_{\text{scat}}(\mu) + 2\frac{M_\pi^2 + M_K^2}{4}L_5(\mu) + \chi_{\pi K}^{1/2}(\mu) \right] \right\} \tag{104}$$

These formulae are written in terms of $\mathcal{O}(p^4)$ values of the masses and decay constants (M_π, M_K, F_π and F_K) of the Nambu-Goldstone bosons (which, in turn, depend on the quark masses). We recall that the "Bernese" normalization for the pion decay constant at the physical point is adopted (cf. footnote 18). The constants $L_5(\mu)$ and

$$L_{\text{scat}}(\mu) = 2L_1(\mu) + 2L_2(\mu) + L_3(\mu) - 2L_4(\mu) - \frac{1}{2}L_5(\mu) + 2L_6(\mu) + L_8(\mu) \tag{105}$$

are the $SU(3)$ low-energy constants (LECs) at the renormalization scale μ. The objects $\chi_{PQ}^{(I)}(\mu)$ are known functions with chiral logarithmic terms and dependence on the scale μ. In

terms of these objects the functions $\chi^I_{PQ}(\mu)$ in Eqs. (101)-(104) read[4]

$$\chi^2_{\pi\pi}(\mu) = \frac{1}{(16\pi)^2}\left[-\frac{3M^2_\pi}{2}\log(\frac{M^2_\pi}{\mu^2}) - \frac{M^2_\pi}{18}\log(\frac{M^2_\eta}{\mu^2}) + \frac{4M^2_\pi}{9}\right],$$ (106)

$$\chi^1_{KK}(\mu) = \frac{1}{(16\pi)^2}\left[\frac{M^2_\pi M^2_K}{4(M^2_K - M^2_\pi)}\log(\frac{M^2_\pi}{\mu^2}) - M^2_K\log(\frac{M^2_K}{\mu^2})\right.$$
$$\left. + \frac{-20M^4_K + 11M^2_\pi M^2_K}{36(M^2_K - M^2_\pi)}\log(\frac{M^2_\eta}{\mu^2}) + \frac{7M^2_K}{9}\right],$$ (107)

$$\chi^{3/2}_{\pi K}(\mu) = \frac{1}{(16\pi)^2}\left[\frac{22M^3_\pi M_K + 11M^2_\pi M^2_K - 5M^4_\pi}{8(M^2_K - M^2_\pi)}\log(\frac{M^2_\pi}{\mu^2})\right.$$
$$+ \frac{9M^4_K - 134M_\pi M^3_K + 16M^3_\pi M_K - 55M^2_\pi M^2_K}{36(M^2_K - M^2_\pi)}\log(\frac{M^2_K}{\mu^2})$$
$$+ \frac{36M^4_K + 48M_\pi M^3_K - 10M^3_\pi M_K + 11M^2_\pi M^2_K - 9M^4_\pi}{72(M^2_K - M^2_\pi)}\log(\frac{M^2_\eta}{\mu^2})$$
$$\left. + \frac{43M_\pi M_K}{9} - \frac{8M_\pi M_K}{9}t_1(M_\pi, M_K)\right],$$ (108)

$$\chi^{1/2}_{\pi K}(\mu) = \frac{1}{(16\pi)^2}\left[\frac{11M^3_\pi M_K - 11M^2_\pi M^2_K + 5M^4_\pi}{4(M^2_K - M^2_\pi)}\log(\frac{M^2_\pi}{\mu^2})\right.$$
$$+ \frac{-9M^4_K - 67M_\pi M^3_K + 8M^3_\pi M_K + 55M^2_\pi M^2_K}{18(M^2_K - M^2_\pi)}\log(\frac{M^2_K}{\mu^2})$$
$$+ \frac{-36M^4_K + 24M^3_K M_\pi - 5M_K M^3_\pi - 11M^2_K M^2_\pi + 9M^4_\pi}{36(M^2_K - M^2_\pi)}\log(\frac{M^2_\eta}{\mu^2})$$
$$\left. + \frac{43M_\pi M_K}{9} + \frac{4M_\pi M_K}{9}t_1(M_\pi, M_K) - \frac{12M_\pi M_K}{9}t_2(M_\pi, M_K)\right],$$ (109)

where $t_1(M_\pi, M_K)$, $t_2(M_\pi, M_K)$ can be written as

$$t_1(M_\pi, M_K) = \frac{\sqrt{(M_K + M_\pi)(2M_K - M_\pi)}}{M_K - M_\pi}\arctan\left(\frac{2(M_K - M_\pi)}{M_K + 2M_\pi}\sqrt{\frac{M_K + M_\pi}{2M_K - M_\pi}}\right),$$ (110)

$$t_2(M_\pi, M_K) = \frac{\sqrt{(M_K - M_\pi)(2M_K + M_\pi)}}{M_K + M_\pi}\arctan\left(\frac{2(M_K + M_\pi)}{M_K - 2M_\pi}\sqrt{\frac{M_K - M_\pi}{2M_K + M_\pi}}\right).$$ (111)

---

[4] There is a typo in the original version of Ref. [30] which made us mistakenly give the last term in the square bracket of Eq. (107) as $\frac{10M^2_K}{9}$ in the arXiv:2111.09849_v1 version of this report. The correct expression with the last term $\frac{7M^2_K}{9}$ agrees with Eq. (32) in [34] which, to the best of our knowledge, is the earliest reference for this quantity. Moreover, in the $SU(3)$ limit $(16\pi)^2\chi^2_{\pi\pi}(\mu) \to -\frac{14}{9}M^2_\pi\log(\frac{M^2_\pi}{\mu^2}) + \frac{4}{9}M^2_\pi$, while the Gell-Mann-Oakes-Renner relation and the substitution $M^2_K = M^2_\pi + \epsilon$ yield $(16\pi)^2\chi^1_{KK}(\mu) \to \frac{M^2_\pi(M^2_\pi + \epsilon)}{4\epsilon}\log(\frac{M^2_\pi}{\mu^2}) - (M^2_\pi + \epsilon)\log(\frac{M^2_\pi + \epsilon}{\mu^2}) + \frac{(M^2_\pi + \epsilon)(-20M^2_\pi - 20\epsilon + 11M^2_\pi)}{36\epsilon}\log(\frac{M^2_\pi + 4\epsilon/3}{\mu^2}) + \frac{7}{9}(M^2_\pi + \epsilon)$. In this expression the terms $O(\epsilon^{-1})$ cancel, and with $\log(\frac{M^2_\pi + 4\epsilon/3}{\mu^2}) = \log(\frac{M^2_\pi}{\mu^2}) + \frac{4\epsilon}{3M^2_\pi}$ one obtains $(16\pi)^2\chi^1_{KK}(\mu) \to -\frac{14}{9}M^2_\pi\log(\frac{M^2_\pi}{\mu^2}) + \frac{4}{9}M^2_\pi$ in the limit $\epsilon \to 0$. Hence $\chi^2_{\pi\pi}(\mu) = \chi^1_{KK}(\mu)$ in the $SU(3)$ limit. We are indebted to André Walker-Loud and Kiyoshi Sasaki for pointing this out to us and for clarifying details, respectively.

In short, these formulae show that – in the $SU(3)$ framework – the four scattering lengths $a_0^1 M_\pi$, $a_0^2 M_K$, $a_0^{3/2} \mu_{\pi K}$, $a_0^{1/2} \mu_{\pi K}$ determine three linear combinations of $L_5(\mu)$ and $L_{\rm scat}(\mu)$. Recall that Eq. (105) shows that the latter object is itself a linear combination of the $L_i(\mu)$. Interestingly, $\pi\pi$ and KK scattering determine the same linear combination $L_{\rm scat}(\mu) - \frac{1}{2}L_5(\mu)$, while $a_0^{3/2} \mu_{\pi K}$ and $a_0^{1/2} \mu_{\pi K}$ determine two more (m_s/m_{ud}-dependent) linear combinations. In the last few lines, we established the habit of omitting the particle subscript in $a_{0,\pi K}^I$ and $a_{0,KK}^I$, since the value of I together with the factor M_π, $\mu_{\pi K}$ or M_K already tells the particles involved in the scattering process. The remaining zero subscript is meant to indicate the S-wave component.

5.2 Extraction of SU(2) low-energy constants

5.2.1 New results for individual LO SU(2) LECs

We are aware of four new papers with results on individual $SU(2)$ LECs plus an additional one which we overlooked in FLAG 19 [3]. They all give results on the LO LECs, B and/or F, where B is frequently traded for the condensate $\Sigma \equiv BF^2$ (both B and Σ are renormalized at the scale $\mu = 2\,{\rm GeV}$). We start by briefly mentioning their details.

The paper ETM 20A [36] presents an $N_f = 2$ calculation with twisted mass fermions, using three pion masses down to the physical value at a single lattice spacing $a = 0.0914(15)\,{\rm fm}$. They report a value of F as given in Tab. 22 and a value of $\bar{\ell}_4$ discussed in Sec. 5.2.2 below. The publication status changed from "preprint" to "accepted" after our closing date (as did the quoted uncertainty). In practical terms this change is insignificant, since the quoted number (due to a red tag) would not contribute to the $N_f = 2$ average.

The paper χQCD 21 [37] employs $N_f = 2 + 1$ QCD with domain wall fermions and RI/MOM renormalization. They have two ensembles with physical pion mass (139 MeV) at lattice spacings $a = 0.114$fm and $a = 0.084$fm, one ensemble with $M_\pi = 234\,{\rm MeV}$ at $a = 0.071$fm, and one with $M_\pi = 371\,{\rm MeV}$ at $a = 0.063$fm that is only used to test the lattice spacing dependence of the scalar renormalization factor. They report the value of $\Sigma^{1/3}$ as listed in Tab. 21.

The paper ETM 21 [38] uses $N_f = 2 + 1 + 1$ flavours of twisted mass fermions, ten ensembles, three lattice spacings ($a = 0.092, 0.080, 0.068$fm), up to four pion masses $M_\pi \in$ [135 MeV, 346 MeV], up to two volumes, and $L(M_{\pi,\min}) = 5.55\,{\rm fm}$. The scale is set by $f_\pi^{\rm phys} = \sqrt{2}F_\pi^{\rm phys} = 130.4(2)\,{\rm MeV}$ [22]. They analyze the quark mass dependence of both F_π and the (chiral and finite-volume) log-free quantity $X_\pi = (F_\pi M_\pi^4)^{1/5}$ [39], to determine F and $\bar{\ell}_4$ in two different ways. The two fitting procedures yield nearly identical results for F. The two central values agree exactly, as do the two systematic uncertainties; only the combined statistical plus fitting uncertainty differs a bit among the two approaches. Since the paper does not give preference to one of the fitting procedures, we take the liberty to condense them, assuming 100% correlation, into the single result $F = 87.7(6)(5)\,{\rm MeV}$ as listed in Tab. 22. They also report a value of $\bar{\ell}_4$ to be mentioned in Sec. 5.2.2 below.

The paper ETM 21A [40] is again based on $N_f = 2 + 1 + 1$ flavours of twisted mass fermions, ten ensembles, three lattice spacings, $a = 0.095, 0.082, 0.069$fm, up to four pion masses $M_\pi \in [134\,{\rm MeV}, 346\,{\rm MeV}]$, up to two volumes, and $L(M_{\pi,\min}) = 5.52\,{\rm fm}$. The scale is set by $f_\pi^{\rm phys} = \sqrt{2}F_\pi^{\rm phys} = 130.4(2)\,{\rm MeV}$ [22], and cross-checked with the nucleon mass. From the analysis of the pion sector they determine values of F and $\Sigma^{1/3}$ as listed in Tab. 22 and Tab. 21, respectively.
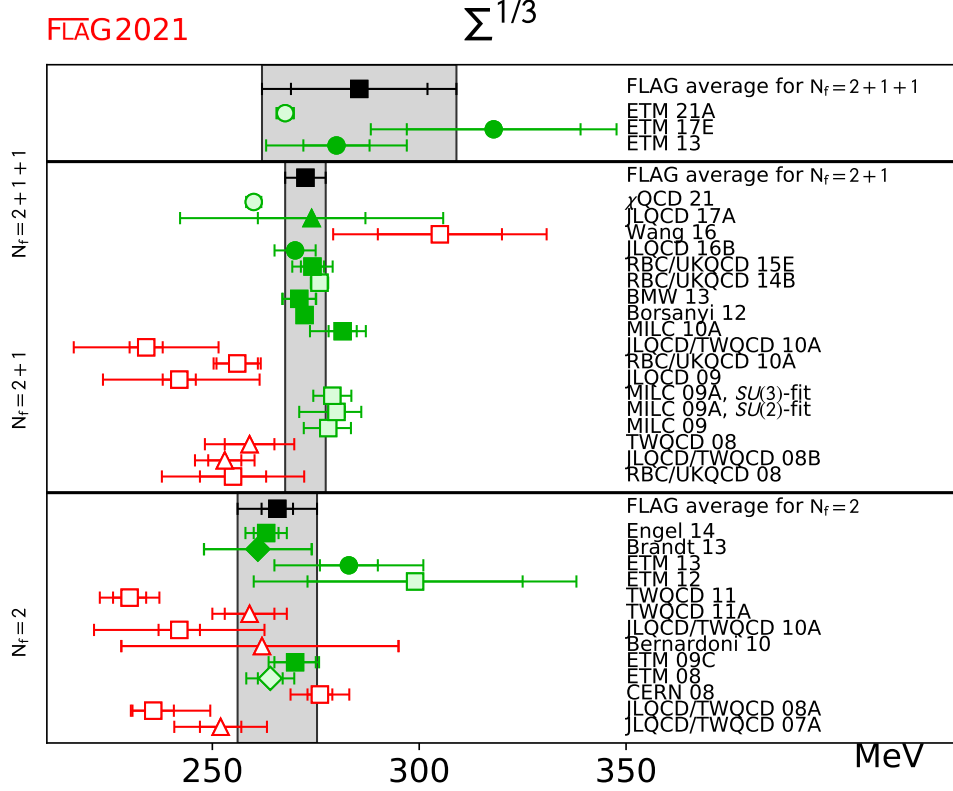
Figure 14: Cubic root of the $SU(2)$ quark condensate $\Sigma \equiv -\lim_{m_u,m_d\to 0}\langle \bar{u}u\rangle$ in the $\overline{\text{MS}}$-scheme, at the renormalization scale $\mu = 2\,\text{GeV}$. Square symbols indicate determinations from correlators in the p-regime, up triangles refer to extractions from the topological susceptibility, diamonds to determinations from the pion form factor, and bullet points refer to the spectral density method.

Finally, we should mention Ref. [41] which, regrettably, escaped our attention when preparing the last FLAG report [3]. The authors extract the quark condensate from an OPE analysis of the Landau-gauge quark propagator. They use overlap valence quarks on three ensembles with (2+1)-flavor domain-wall fermions with $a^{-1} = 1.75\,\text{GeV}$ and sea pion masses of 331, 419 and 557 MeV from the RBC/UKQCD collaboration. Their eight valence pion masses range from 220 to 600 MeV. Their result for $\Sigma^{1/3}$ is listed in Tab. 21. With only a single lattice spacing, their result does not contribute to the FLAG average.

Perhaps it is worth comparing the results for $f \equiv \sqrt{2}F$ in Refs. [38, 40]. Carrying all errors along, one finds $\Delta f[\text{MeV}] = 124.0(0.9)(0.7) - 122.82(32)(65) = 1.18(1.35)$, which is less than one standard deviation. Given that the two studies were carried out on largely the same ensemble basis, it is perhaps reasonable to assume the statistical error is $\sim 100\%$ correlated. In this case, the difference would be $\Delta f[\text{MeV}] = 124.0(0.7) - 122.82(65) = 1.18(0.96)$, which is 1.24σ and thus perfectly acceptable. The chiral analysis in the two papers is treated somewhat differently, which would lead to differences in the neglected NNLO terms, and thus reflects a systematic effect.

The new results for $\Sigma^{1/3}$ and F_π/F, together with the previous ones, are shown in Fig. 14 and Fig. 15, respectively.

Collaboration	Ref.	N_f	publication status	chiral extrapolation	cont. extrapolation	finite volume	renormalization	$\Sigma^{1/3}$
ETM 21A	[40]	2+1+1	P	★	○	★	★	267.6(1.8)(1.1)
ETM 17E	[42]	2+1+1	A	○	★	○	★	318(21)(21)
ETM 13	[43]	2+1+1	A	○	★	★	★	280(8)(15)
χQCD 21	[37]	2+1	P	★	★	★	★	260.3(0.7)(1.7)
JLQCD 17A	[44]	2+1	A	○	★	★	★	274(13)(29)
Wang 16	[41]	2+1	A	○	■	■	★	305(15)(21)
JLQCD 16B	[85]	2+1	A	○	★	★	★	270.0(1.3)(4.8)
RBC/UKQCD 15E	[46]	2+1	A	★	★	★	★	274.2(2.8)(4.0)
RBC/UKQCD 14B	[47]	2+1	A	★	★	★	★	275.9(1.9)(1.0)
BMW 13	[48]	2+1	A	★	★	★	★	271(4)(1)
Borsanyi 12	[49]	2+1	A	○	○	★	★	272.3(1.2)(1.4)
JLQCD/TWQCD 10A	[50]	2+1	A	★	■	■	★	234(4)(17)
MILC 10A	[51]	2+1	C	○	★	★	○	281.5(3.4)$\left(^{+2.0}_{-5.9}\right)$(4.0)
RBC/UKQCD 10A	[52]	2+1	A	○	○	■	★	256(5)(2)(2)
JLQCD 09	[53]	2+1	A	★	■	■	★	242(4)$\left(^{+19}_{-18}\right)$
MILC 09A, $SU(3)$-fit	[54]	2+1	C	○	★	★	○	279(1)(2)(4)
MILC 09A, $SU(2)$-fit	[54]	2+1	C	○	★	★	○	280(2)$\left(^{+4}_{-8}\right)$(4)
MILC 09	[55]	2+1	A	○	★	★	○	278(1)$\left(^{+2}_{-3}\right)$(5)
TWQCD 08	[56]	2+1	A	■	■	■	★	259(6)(9)
PACS-CS 08, $SU(3)$-fit	[57]	2+1	A	★	■	■	■	312(10)
PACS-CS 08, $SU(2)$-fit	[57]	2+1	A	★	■	■	■	309(7)
RBC/UKQCD 08	[58]	2+1	A	○	■	○	★	255(8)(8)(13)
Engel 14	[59]	2	A	★	★	★	★	263(3)(4)
Brandt 13	[60]	2	A	○	★	○	★	261(13)(1)
ETM 13	[43]	2	A	○	★	○	★	283(7)(17)
ETM 12	[61]	2	A	○	★	○	★	299(26)(29)
Bernardoni 11	[62]	2	C	○	■	■	★	306(11)
TWQCD 11	[63]	2	A	○	■	■	★	230(4)(6)
TWQCD 11A	[64]	2	A	○	■	■	★	259(6)(7)
JLQCD/TWQCD 10A	[50]	2	A	★	■	■	★	242(5)(20)
Bernardoni 10	[65]	2	A	○	■	■	★	262$\left(^{+33}_{-34}\right)\left(^{+4}_{-5}\right)$
ETM 09C	[66]	2	A	○	★	○	★	270(5)$\left(^{+3}_{-4}\right)$
ETM 08	[67]	2	A	○	○	○	★	264(3)(5)
CERN 08	[68]	2	A	○	■	○	★	276(3)(4)(5)
Hasenfratz 08	[69]	2	A	○	■	○	★	248(6)
JLQCD/TWQCD 08A	[70]	2	A	○	■	■	★	235.7(5.0)(2.0)$\left(^{+12.7}_{-0.0}\right)$
JLQCD/TWQCD 07	[71]	2	A	○	■	■	★	239.8(4.0)
JLQCD/TWQCD 07A	[72]	2	A	★	■	■	★	252(5)(10)

Table 21: Cubic root of the $SU(2)$ quark condensate $\Sigma \equiv -\lim_{m_u,m_d\to 0}\langle \bar{u}u \rangle$ in MeV units, in the $\overline{\text{MS}}$-scheme, at the renormalization scale $\mu = 2\,\text{GeV}$. All ETM values that were available only in r_0 units were converted on the basis of $r_0 = 0.48(2)\,\text{fm}$ [73–75], with this error being added in quadrature to any existing systematic error.

Collaboration	Ref.	N_f	publication status	chiral extrapolation	cont. extrapolation	finite volume	F	F_π/F
ETM 21A	[40]	2+1+1	P	★	○	★	86.85(23)(46)	*1.062(3)(6)*
ETM 21	[38]	2+1+1	P	★	○	★	87.7(6)(5)	*1.051(7)(6)*
ETM 11	[76]	2+1+1	C	○	★	○	85.60(4)*(13)*	*1.077(2)(2)*
ETM 10	[77]	2+1+1	A	○	■	★	85.66(6)(13)	*1.076(2)(2)*
RBC/UKQCD 15E	[46]	2+1	A	★	★	★	85.8(1.1)(1.5)	1.0641(21)(49)
RBC/UKQCD 14B	[47]	2+1	A	★	★	★	86.63(12)(13)	1.0645(15)(0)
BMW 13	[48]	2+1	A	★	★	★	88.0(1.3)(0.3)	1.055(7)(2)
Borsanyi 12	[49]	2+1	A	○	○	★	86.78(05)(25)	1.0627(06)(27)
NPLQCD 11	[78]	2+1	A	○	○	○	$86.8(2.1)\binom{+3.3}{-3.4}$	$1.062(26)\binom{+42}{-40}$
MILC 10	[79]	2+1	C	○	★	★	87.0(4)(5)	*1.060(5)(6)*
MILC 10A	[51]	2+1	C	○	★	★	$87.5(1.0)\binom{+0.7}{-2.6}$	$1.054(12)\binom{+31}{-09}$
MILC 09A, $SU(3)$-fit	[54]	2+1	C	○	★	★	86.8(2)(4)	1.062(1)(3)
MILC 09A, $SU(2)$-fit	[54]	2+1	C	○	★	★	$87.4(0.6)\binom{+0.9}{-1.0}$	$1.054(7)\binom{+12}{-11}$
MILC 09	[55]	2+1	A	○	★	★	$87.66(17)\binom{+28}{-52}$	$1.052(2)\binom{+6}{-3}$
PACS-CS 08, $SU(3)$-fit	[57]	2+1	A	★	■	■	90.3(3.6)	1.062(8)
PACS-CS 08, $SU(2)$-fit	[57]	2+1	A	★	■	■	89.4(3.3)	1.060(7)
RBC/UKQCD 08	[58]	2+1	A	○	■	○	81.2(2.9)(5.7)	1.080(8)
ETM 20A	[36]	2	A	★	■	○	86.46(0.06)(2.40)	*1.067(1)(30)*
ETM 15A	[75]	2	A	★	■	○	86.3(2.8)	*1.069(35)*
Engel 14	[59]	2	A	★	★	★	85.8(0.7)(2.0)	1.075(09)(25)
Brandt 13	[60]	2	A	○	★	○	84(8)(2)	1.080(16)(6)
QCDSF 13	[80]	2	A	★	○	○	86(1)	*1.07(1)*
TWQCD 11	[63]	2	A	○	■	■	83.39(35)(38)	1.106(5)(5)
ETM 09C	[66]	2	A	○	★	○	$85.91(07)\binom{+78}{-07}$	$1.0755(6)\binom{+08}{-94}$
ETM 08	[67]	2	A	○	○	○	86.6(7)(7)	1.067(9)(9)
Hasenfratz 08	[69]	2	A	○	■	○	90(4)	*1.02(5)*
JLQCD/TWQCD 08A	[70]	2	A	○	■	■	$79.0(2.5)(0.7)\binom{+4.2}{-0.0}$	$1.167(37)(10)\binom{+02}{-62}$
JLQCD/TWQCD 07	[71]	2	A	○	■	■	87.3(5.6)	*1.06(7)*
Colangelo 03	[81]						86.2(5)	1.0719(52)

Table 22: Results for the $SU(2)$ low-energy constant F (in MeV) and for the ratio F_π/F. All ETM values that were available only in r_0 units were converted on the basis of $r_0 = 0.48(2)\,$fm [73–75], with this error being added in quadrature to any existing systematic error. Numbers in slanted fonts have been calculated by us, based on $\sqrt{2}F_\pi^{\rm phys} = 130.41(20)\,$MeV [22], with this error being added in quadrature to any existing systematic error (otherwise to the statistical error). The systematic error in ETM 11 has been carried over from ETM 10.
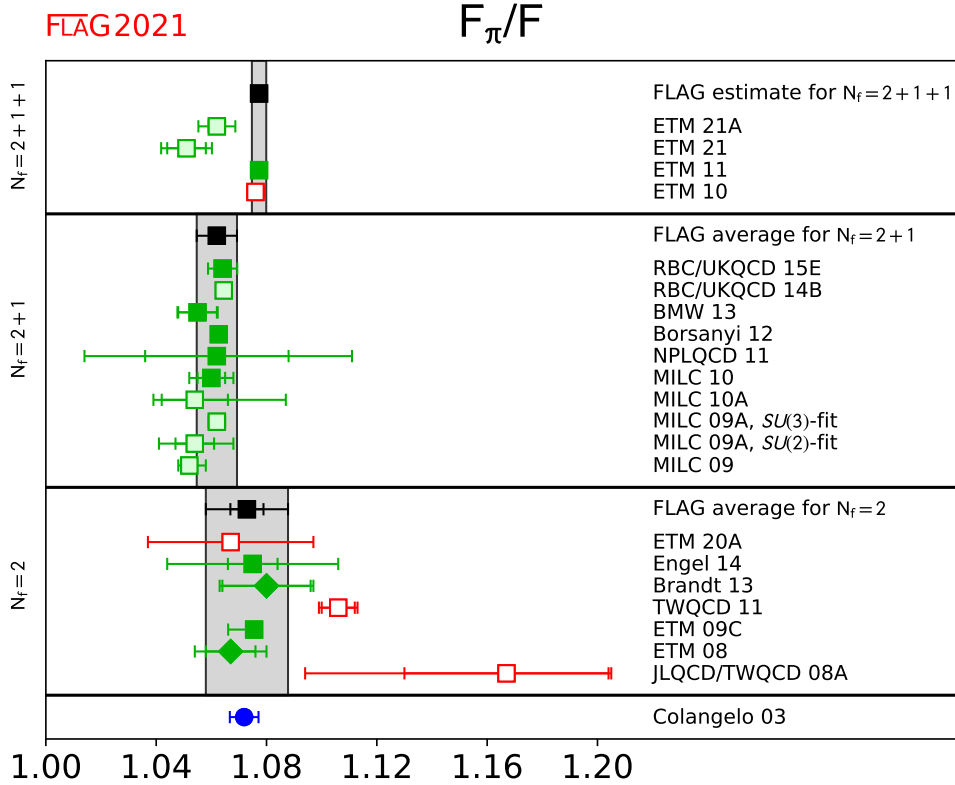
Figure 15: Comparison of the results for the ratio of the physical pion decay constant F_π and the leading-order $SU(2)$ low-energy constant F. Square symbols indicate determinations from correlators in the p-regime, and diamonds from the pion form factor.

5.2.2 New results for individual NLO SU(2) LECs

Two of the aforementioned papers contain new results on $\bar{\ell}_4$, i.e., a specific LEC at NLO of the $SU(2)$ framework. ETM 20A [36] quotes $\bar{\ell}_4 = 4.31(4)(2)(11)(5)$ for $N_f = 2$, while ETM 21 [38] finds $\bar{\ell}_4 = 3.44(28)(36)$ for $N_f = 2 + 1 + 1$. These results are listed in Tab. 23.

If one were to ignore N_f, the two new results would appear inconsistent. While an implicit dependence on the strange- (and highly suppressed) charm-quark mass in the sea is a logical possibility, it seems to us these results should be considered in conjunction with the FLAG 19 averages for the quantity $\bar{\ell}_4$. The FLAG 19 average for $N_f = 2$, based on four papers, was 4.40(28), the average for $N_f = 2 + 1$, based on five papers, was 4.02(45), and the estimate for $N_f = 2 + 1 + 1$, based on a single paper, was 4.73(10). In terms of standard deviations the difference "old average minus new result" is $4.40(28) - 4.31(13) = 0.09(31)$ or 0.3σ for $N_f = 2$, while it is $4.73(10) - 3.44(46) = 1.29(47)$ or 2.7σ for $N_f = 2 + 1 + 1$. Hence, the new $N_f = 2$ result of ETM 20A [36] is in perfect agreement with the corresponding FLAG 19 average. On the other hand, the new $N_f = 2 + 1 + 1$ result of ETM 21 [38] is largely *inconsistent* with the corresponding FLAG 19 estimate, which was taken from Ref. [76]. Perhaps one should take a step back at this point, and consider the option that the implicit N_f-dependence (through a dynamical strange and charm quark) is smaller than some unaccounted-for systematic effects in at least one of the works considered. On the practial side neither one of the new results qualifies for a FLAG average (ETM 20A [36] has a red tag, ETM 21 [38] is still unpublished).

Collaboration	Ref.	N_f	publication status	chiral extrapolation	cont. extrapolation	finite volume	$\bar{\ell}_3$	$\bar{\ell}_4$
ETM 21	[38]	2+1+1	P	★	○	★		3.44(28)(36)
ETM 11	[76]	2+1+1	C	○	★	○	3.53(5)(26)	4.73(2)(10)
ETM 10	[77]	2+1+1	A	○	■	★	3.70(7)(26)	4.67(3)(10)
RBC/UKQCD 15E	[46]	2+1	A	★	★	★	2.81(19)(45)	4.02(8)(24)
RBC/UKQCD 14B	[47]	2+1	A	★	★	★	2.73(13)(0)	4.113(59)(0)
BMW 13	[48]	2+1	A	★	★	★	2.5(5)(4)	3.8(4)(2)
RBC/UKQCD 12	[82]	2+1	A	★	○	★	2.91(23)(07)	3.99(16)(09)
Borsanyi 12	[49]	2+1	A	○	○	★	3.16(10)(29)	4.03(03)(16)
NPLQCD 11	[78]	2+1	A	○	○	○	$4.04(40)\binom{+73}{-55}$	$4.30(51)\binom{+84}{-60}$
MILC 10	[79]	2+1	C	○	★	★	3.18(50)(89)	4.29(21)(82)
MILC 10A	[51]	2+1	C	○	★	★	$2.85(81)\binom{+37}{-92}$	$3.98(32)\binom{+51}{-28}$
RBC/UKQCD 10A	[52]	2+1	A	○	○	■	2.57(18)	3.83(9)
MILC 09A, $SU(3)$-fit	[54]	2+1	C	○	★	★	3.32(64)(45)	4.03(16)(17)
MILC 09A, $SU(2)$-fit	[54]	2+1	C	○	★	★	$3.0(6)\binom{+9}{-6}$	3.9(2)(3)
PACS-CS 08, $SU(3)$-fit	[57]	2+1	A	★	■	■	3.47(11)	4.21(11)
PACS-CS 08, $SU(2)$-fit	[57]	2+1	A	★	■	■	3.14(23)	4.04(19)
RBC/UKQCD 08	[58]	2+1	A	○	■	○	3.13(33)(24)	4.43(14)(77)
ETM 20A	[36]	2	A	★	■	○		4.31(4)(2)(11)(5)
ETM 15A	[75]	2	A	★	■	○		3.3(4)
Gülpers 15	[83]	2	A	★	★	★		4.54(30)(0)
Gülpers 13	[84]	2	A	○	■	○		4.76(13)
Brandt 13	[60]	2	A	○	★	○	3.0(7)(5)	4.7(4)(1)
QCDSF 13	[80]	2	A	★	○	○		4.2(1)
Bernardoni 11	[62]	2	C	○	■	■	4.46(30)(14)	4.56(10)(4)
TWQCD 11	[63]	2	A	○	■	■	4.149(35)(14)	4.582(17)(20)
ETM 09C	[66]	2	A	○	★	○	$3.50(9)\binom{+09}{-30}$	$4.66(4)\binom{+04}{-33}$
JLQCD/TWQCD 09	[85]	2	A	○	■	■		4.09(50)(52)
ETM 08	[67]	2	A	○	○	○	3.2(8)(2)	4.4(2)(1)
JLQCD/TWQCD 08A	[70]	2	A	○	■	■	$3.38(40)(24)\binom{+31}{-00}$	$4.12(35)(30)\binom{+31}{-00}$
CERN-TOV 06	[86]	2	A	○	■	■	3.0(5)(1)	
Colangelo 01	[7]							4.4(2)
Gasser 84	[1]						2.9(2.4)	4.3(9)

Table 23: Results for the $SU(2)$ NLO low-energy constants $\bar{\ell}_3$ and $\bar{\ell}_4$. For comparison, the last two lines show results from phenomenological analyses. The systematic error in ETM 11 has been carried over from ETM 10.
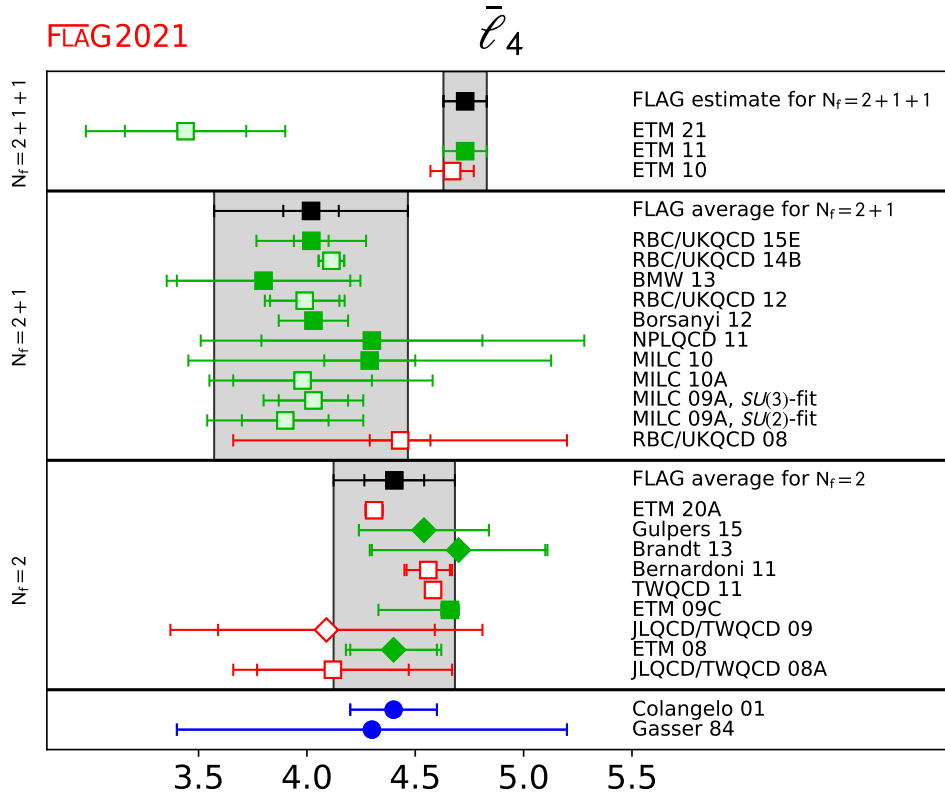
Figure 16: Effective coupling constant $\bar{\ell}_4$. Squares indicate determinations from correlators in the p-regime, diamonds refer to determinations from the pion form factor.

In summary, the time is not ripe to give an update on the $\bar{\ell}_4$ average given in FLAG 19.

The two new results on $\bar{\ell}_4$ in Tab. 23 are displayed in Fig. 16, along with all previous determinations with systematic error bars. Since there is no new entry in the first column of the table, there is no analogous figure for $\bar{\ell}_3$.

There is also new information on $\bar{\ell}_6$. It appears in three new papers on the slope of the vector form factor at $q^2 = 0$ ("charge radius") of the pion. We follow our tradition of quoting and comparing results in terms of $\langle r^2 \rangle_V^\pi$ rather than $\bar{\ell}_6$. As mentioned before, we start with a brief discussion of the particulars of these papers.

The paper Feng 19 [90] is based on $N_f = 2 + 1$ flavours of domain-wall valence quarks on domain-wall sea. This collaboration uses four ensembles essentially at the physical mass point[5] and another one at $M_\pi = 341$ MeV. At the physical mass point they have three lattice spacings in the range $a^{-1} = 1.015 - 1.73$ GeV, i.e., none of them satisfies $a < 0.1$fm. The respective box sizes are $L = [6.22, 4.58, 5.48]$fm, hence $L(M_{\pi,\mathrm{min}}) = 6.22$fm.

The paper χQCD 20 [89] employs overlap valence quarks on $N_f = 2 + 1$ ensembles with domain-wall sea quarks. They use a total of seven ensembles, with three of them being at the physical point. They cover five lattice spacings $a = 0.083 - 0.195$fm, of which only one is below 0.1fm. The relevant box size is 6.24fm at the physical point, where they have $M_\pi L = 4.45$.

---

[5]This earns them a green box on "chiral extrapolation", but the criterion was crafted with the idea of a global fit which takes all available information into account. In the setup of Feng 19 [90] it is barely possible to disentangle a small M_π dependence in the vicinity of M_π^{phys} from cut-off effects.

Collaboration	Ref.	N_f	publication status	chiral extrapolation	continuum extrapolation	finite volume	$\langle r^2 \rangle_V^\pi$ [fm^2]	$\bar{\ell}_6$
HPQCD 15B	[87]	2+1+1	A	★	○	★	0.403(18)(6)	
Gao 21	[88]	2+1	P	○	■	★	0.42(2)$_{\text{tot}}$	
χQCD 20	[89]	2+1	A	★	○	★	0.430(5)(13)	17.1(1.4)
Feng 19	[90]	2+1	A	★	■	★	0.434(20)(13)	
JLQCD 15A, $SU(2)$-fit	[91]	2+1	A	○	■	○	0.395(26)(32)	13.49(89)(82)
JLQCD 14	[92]	2+1	A	★	■	■	0.49(4)(4)	7.5(1.3)(1.5)
PACS-CS 11A	[93]	2+1	A	○	■	○	0.441(46)	
RBC/UKQCD 08A	[94]	2+1	A	■	■	○	0.418(31)	12.2(9)
LHP 04	[95]	2+1	A	■	■	■	0.310(46)	
ETM 17F	[96]	2	A	★	■	★	0.443(21)(20)	16.21(76)(70)
Brandt 13	[60]	2	A	○	★	○	0.481(33)(13)	15.5(1.7)(1.3)
JLQCD/TWQCD 09	[85]	2	A	○	■	■	0.409(23)(37)	11.9(0.7)(1.0)
ETM 08	[67]	2	A	○	○	○	0.456(30)(24)	14.9(1.2)(0.7)
QCDSF/UKQCD 06A	[97]	2	A	○	★	■	0.441(19)(63)	
Bijnens 98	[98]						0.437(16)	16.0(0.5)(0.7)
NA7 86	[99]						0.439(8)	
Gasser 84	[1]							16.5(1.1)

Table 24: Vector form factor of the pion: Lattice results for the charge radius $\langle r^2 \rangle_V^\pi$ and the chiral coupling constant $\bar{\ell}_6$ are compared with the experimental value, as obtained by NA7, and some phenomenological estimates. The publication status of χQCD 20 [89] changed from "preprint" to "accepted" after our closing date.

Renormalization is done nonperturbatively.

The paper Gao 21 [88] is based on $N_f = 2 + 1$ HISQ (staggered) ensembles on which they invert clover valence quarks. They have $M_{\pi,\text{sea}} = M_{\pi,\text{val}} = 140\,\text{MeV}$ at $a = 0.076\text{fm}$ in a $64^3 \times 64$ volume. In addition, they have $M_{\pi,\text{sea}} = 160\,\text{MeV}$, $M_{\pi,\text{val}} = 300\,\text{MeV}$ at $a = 0.06\text{fm}$ (in a $48^3 \times 64$ box), and essentially the same sea-valence mass combination at $a = 0.04\text{fm}$ (in a $64^3 \times 64$ box). The vector form factor is renormalized nonperturbatively. Unfortunately, no continuum extrapolation is performed; they quote the result from the $a \simeq 0.076\text{fm}$ physical pion mass ensemble as listed in Tab. 24. The error quoted is a total error, comprising systematic uncertainties unrelated to cut-off effects.

The available information on $\langle r^2 \rangle_V^\pi$ is summarized in Fig. 17. It is obvious that the lattice computations for this quantity do not achieve the precision of the experimental result (NA 7) yet.
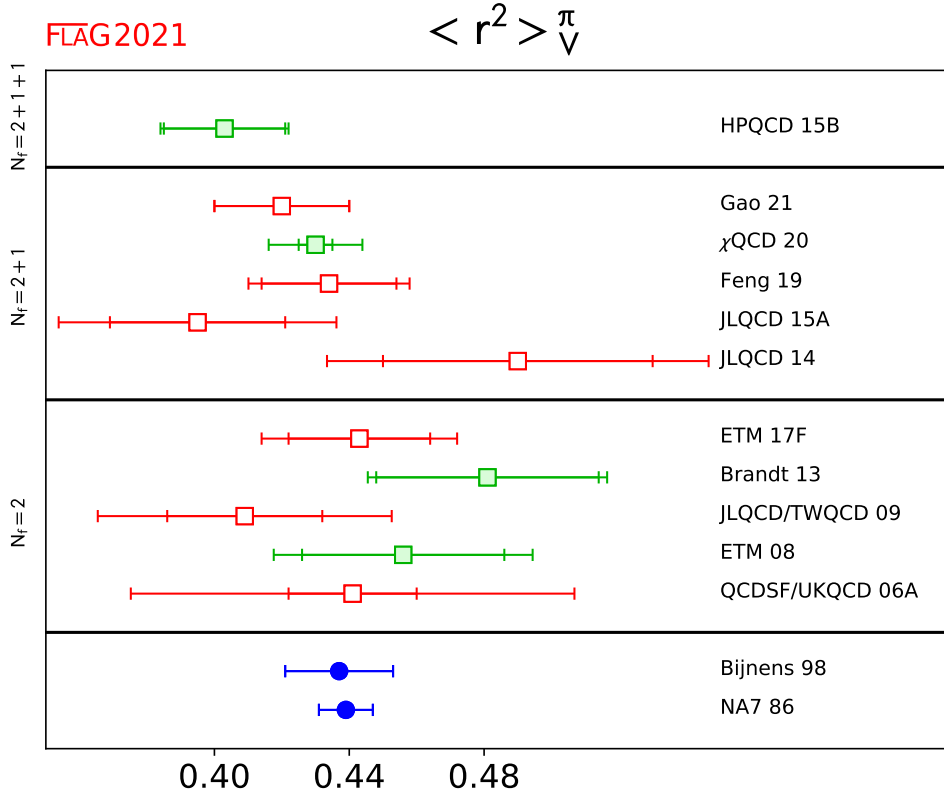
Figure 17:   Summary of the pion form factor $\langle r^2 \rangle_V^\pi$. The publication status of χQCD 20 [89] changed from "preprint" to "accepted" after our closing date.

5.2.3   New results for an SU(2) linear combination linked to $\pi\pi$ scattering

We are aware of four new papers on $\pi\pi$ scattering (in the isospin $I = 2$ and/or $I = 0$ state). As before, we begin with a brief description of their specifics.

Reference [100] by B. Hörz and A. Hanlon uses one CLS ensemble of $N_f = 2 + 1$ nonperturbatively improved Wilson (clover) fermions. Since it is away from the physical mass point and no extrapolation to the latter is attempted, we refrain from applying the FLAG criteria, and there will be no listing in tables and/or plots. We add that this procedure is in strict analogy to our treatment of Ref. [101] in FLAG 19. A sequel publication, based on the same data, is Ref. [102]. They find that the $\pi\pi$ ($I = 2$) spectrum is fit well by an S-wave phase shift that incorporates the expected Adler zero. Obviously, the same comment regarding the applicability of the FLAG criteria applies.

The paper Culver 19 [103] uses $N_f = 2$ flavours of nHYP clover fermions at $a = 0.12$fm, $M_\pi = 315$ MeV on $48 \times 24^2 \times \{24, 30, 48\}$ and $M_\pi = 226$ MeV on $64 \times 24^2 \times \{24, 28, 32\}$. With a conventional analysis technique they find $a_0^2 M_\pi = -0.0455(16)$, after extrapolation to physical pion mass. From an inverse amplitude method, they obtain $a_0^2 M_\pi = -0.0436\left(^{+0.0013}_{-0.0012}\right)$, again at the physical pion mass. Since the paper does not give preference to one of the analysis methods, we take the liberty to condense the two numbers into the result $a_0^2 M_\pi = -0.0445(14)(19)$, as shown in Tab. 25. Here, the systematic error reflects the full difference between the two central values given in the paper.

The paper Mai 19 [104] employs $N_f = 2$ nHYP clover fermions at a single lattice spacing ($a = 0.12$fm), with $M_\pi = 315$ MeV on $48 \times 24^2 \times \{24, 30, 48\}$ lattices and $M_\pi = 224$ MeV on $64 \times 24^2 \times \{24, 28, 32\}$ lattices. They quote, extrapolated to the physical pion mass, $a_0^0 M_\pi = 0.2132\left(^{+0.0008}_{-0.0009}\right)$ and $a_0^2 M_\pi = -0.0433 \pm 0.0002$ for $I = 0$ and $I = 2$, respectively. With statistical error only, these results go into Tab. 25, but not into a plot.

The paper ETM 20B [105] is based on $N_f = 2$ QCD with twisted mass fermions at $a = 0.0914(15)$fm, and with $c_{\mathrm{SW}} = 1.57551$. They have three pion masses ($M_\pi = 340$ MeV on $32^3 \times 64$ and $M_\pi = 242$ MeV and $M_\pi = 134$ MeV on $48^3 \times 96$). They find, for $I = 2$, at the pion masses considered, $a_0^2 M_\pi = -0.2061(49), -0.156(15), -0.0481(86)$, with the last being at physical pion mass, but finite a. Accordingly, we take $a_0^2 M_\pi = -0.0481(86)$ with unknown systematic error. With statistical error only, this result goes into Tab. 25, but not into a plot.

These four works, when combined with the information listed in FLAG 19, represent the information from the lattice on the $\pi\pi$ scattering lengths a_0^0 and a_0^2 in the isopin channels $I = 0$ and $I = 2$, respectively. As can be seen from Eqs. (93, 95), the $I = 0$ scattering length carries information about $\frac{20}{21}\bar{\ell}_1 + \frac{40}{21}\bar{\ell}_2 - \frac{5}{14}\bar{\ell}_3 + 2\bar{\ell}_4$. And from Eqs. (94, 96) it follows that the $I = 2$ counterpart carries information about the linear combination $\frac{4}{3}\bar{\ell}_1 + \frac{8}{3}\bar{\ell}_2 - \frac{1}{2}\bar{\ell}_3 - 2\bar{\ell}_4$. Still, we prefer quoting the dimensionless products $a_0^I M_\pi$ (at the physical mass point) over the aforementioned linear combinations to ease comparison with phenomenology.

The updated Tab. 25 summarizes the present lattice information on $a_0^{I=0} M_\pi$ and $a_0^{I=2} M_\pi$ at the physical mass point, and the results are displayed in Fig. 18. We remind the reader that a lattice computation of $a_0^{I=0} M_\pi$ involves quark-loop disconnected contributions, which tend to be very noisy and thus require large statistics. Compared to the situation in FLAG 19 the number of computations has increased from three to five, but still none of them is free of red tags. The situation is somewhat better for $a_0^{I=2} M_\pi$ which is computed from quark-line connected contributions only. In this case there is one computation at $N_f = 2$ and one at $N_f = 2 + 1 + 1$ that qualifies for a FLAG average. We quote these numbers in subsection 5.2.4 below.

The available information on $a_0^{I=0} M_\pi$ and $a_0^{I=2} M_\pi$ is summarized in Fig. 18. It is obvious that the former quantity (due to quark-loop disconnected contributions) is much harder to calculate on the lattice than the latter one. Nonetheless, the good news is that in both cases the lattice determinations are in reasonable agreement with EFT results.

5.2.4   LO and NLO SU(2) estimates and averages

As promised in an earlier section, here we list our FLAG 19 estimates and averages [3] that all remain unchanged. We refer the reader to that review for details and explanations.

For the $SU(2)$ LEC Σ, in the $\overline{\mathrm{MS}}$ scheme, at the renormalization scale $\mu = 2$ GeV, we obtained the averages and/or estimate

$$
\begin{aligned}
N_f = 2 + 1 + 1: &\qquad \Sigma^{1/3} = 286(23)\,\mathrm{MeV} &\qquad \text{Refs. [42, 43]}, \\
N_f = 2 + 1: &\qquad \Sigma^{1/3} = 272(5)\,\mathrm{MeV} &\qquad \text{Refs. [44, 46, 48, 49, 51, 85]}, \qquad (112) \\
N_f = 2: &\qquad \Sigma^{1/3} = 266(10)\,\mathrm{MeV} &\qquad \text{Refs. [43, 59, 60, 66]},
\end{aligned}
$$

where the errors include both statistical and systematic uncertainties.

For the ratio of the pion decay constant at the physical point, F_π, to its value in the $SU(2)$ chiral limit (zero up- and down-quark mass but physical strange-quark mass), F, we

Collaboration	Ref.	N_f	publication status	chiral extrapolation	cont. extrapolation	finite volume	$a_0^0 M_\pi$	$\ell_{\pi\pi}^0$
Fu 17	[106]	2+1	A	■	○	★	0.217(9)(5)	45.6(7.6)(3.8)
Fu 13	[19]	2+1	A	■	■	★	0.214(4)(7)	43.2(3.5)(5.6)
Fu 11	[107]	2+1	A	■	■	★	0.186(2)	18.7(1.2)
Mai 19	[104]	2	P	■	■	○	0.2132(9)	
ETM 16C	[21]	2	A	★	■	★	0.198(9)(6)	30(8)(6)
Caprini 11	[16]						0.2198(46)(16)(64)	
Colangelo 01	[7]						$0.220(5)_{\rm tot}$	

Collaboration	Ref.	N_f	publication status	chiral extrapolation	cont. extrapolation	finite volume	$a_0^2 M_\pi$	$\ell_{\pi\pi}^2$
ETM 15E	[20]	2+1+1	A	○	★	★	$-0.0442(2)\binom{4}{0}$	$3.79(0.61)\binom{+1.34}{-0.11}$
PACS-CS 13	[30]	2+1	A	★	■	■	−0.04243(22)(43)	
Fu 13	[19]	2+1	A	■	■	★	−0.04430(25)(40)	3.27(0.77)(1.12)
Fu 11	[107]	2+1	A	■	■	★	−0.0416(2)	11.6(9)
NPLQCD 11A	[108]	2+1	A	■	■	★	−0.0417(07)(02)(16)	
NPLQCD 07	[17]	2+1	A	■	■	■	$-0.04330(42)_{\rm tot}$	
NPLQCD 05	[109]	2+1	A	■	■	■	−0.0426(06)(03)(18)	
ETM 20B	[105]	2	A	○	■	○	−0.0481(86)	
Mai 19	[104]	2	P	■	■	○	−0.0433(2)	
Culver 19	[103]	2	P	■	■	○	−0.0445(14)(19)	
Yagi 11	[110]	2	P	○	■	■	−0.04410(69)(18)	
ETM 09G	[18]	2	A	○	○	○	−0.04385(28)(38)	4.65(0.85)(1.07)
CP-PACS 04	[111]	2	A	■	■	★	−0.0413(29)	
Caprini 11	[16]						−0.0445(11)(4)(8)	
Colangelo 01	[7]						$-0.0444(10)_{\rm tot}$	

Table 25: Summary of $\pi\pi$ scattering data in the $I = 0$ (top) and $I = 2$ (bottom) channels. Some of the results have been adapted to our sign convention. The results of Refs. [7, 16] allow for a cross-check with phenomenology.
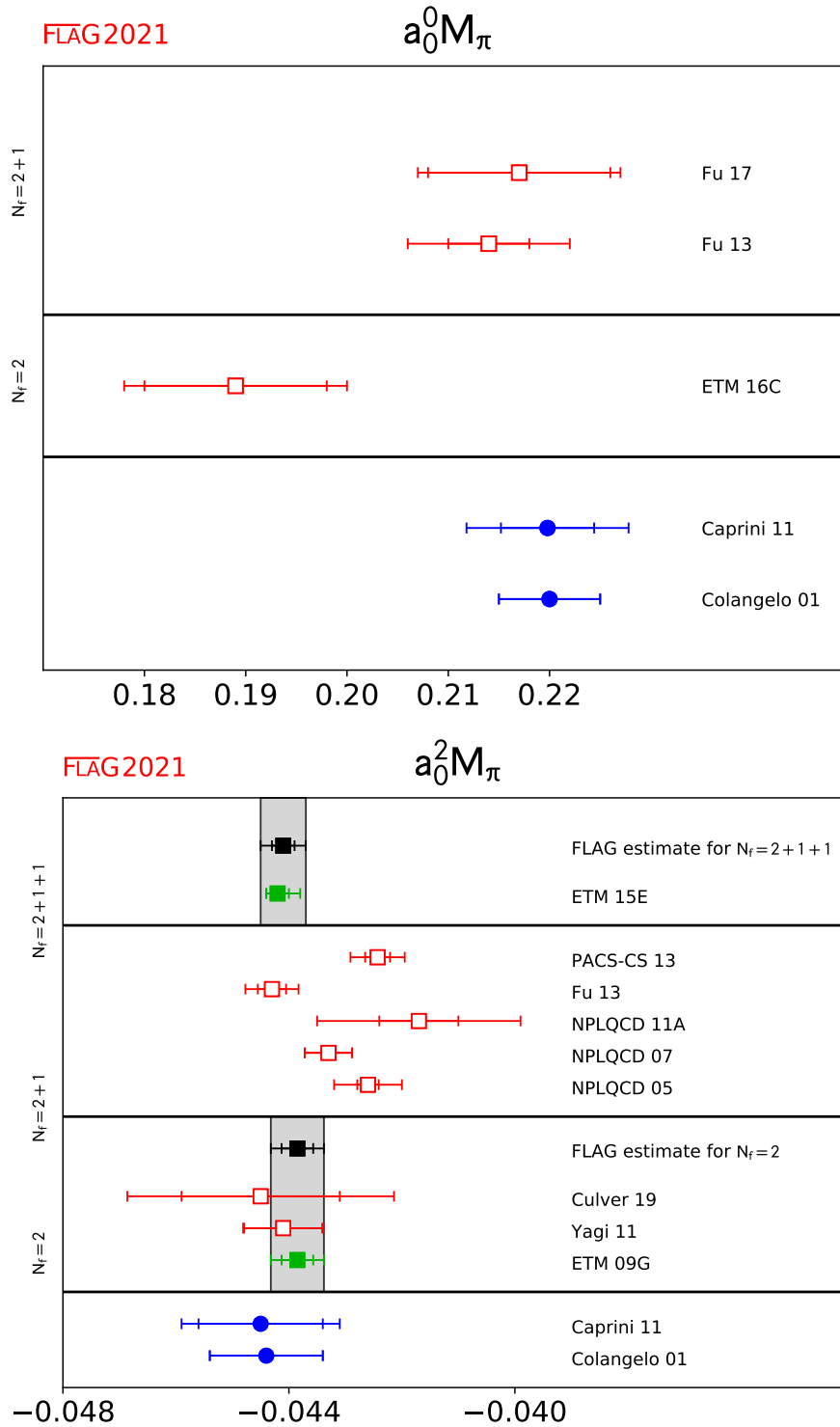
Figure 18: Summary of the $\pi\pi$ scattering lengths $a_0^0 M_\pi$ (top) and $a_0^2 M_\pi$ (bottom). Results in Tab. 25 with statistical error only are not shown.

obtained the averages and/or estimate

$$
\begin{array}{llll}
N_f = 2+1+1: & F_\pi/F = 1.077(3) & \text{Refs. [76],} & \\
N_f = 2+1: & F_\pi/F = 1.062(7) & \text{Refs. [46, 48, 49, 78, 79],} & (113) \\
N_f = 2: & F_\pi/F = 1.073(15) & \text{Refs. [59, 60, 66, 67].} &
\end{array}
$$

For $SU(2)$ NLO LECs we obtained the averages and/or estimates

$$
\begin{array}{llll}
N_f = 2+1+1: & \bar{\ell}_3 = 3.53(26) & \text{Refs. [76],} & \\
N_f = 2+1: & \bar{\ell}_3 = 3.07(64) & \text{Refs. [46, 48, 49, 78, 79],} & (114) \\
N_f = 2: & \bar{\ell}_3 = 3.41(82) & \text{Refs. [60, 66, 67],} &
\end{array}
$$

$$
\begin{array}{llll}
N_f = 2+1+1: & \bar{\ell}_4 = 4.73(10) & \text{Refs. [76],} & \\
N_f = 2+1: & \bar{\ell}_4 = 4.02(45) & \text{Refs. [46, 48, 49, 78, 79],} & (115) \\
N_f = 2: & \bar{\ell}_4 = 4.40(28) & \text{Refs. [60, 66, 67, 83],} &
\end{array}
$$

as well as the estimate

$$
N_f = 2: \qquad \bar{\ell}_6 = 15.1(1.2) \qquad \text{Refs. [60, 67].} \tag{116}
$$

For the scattering length extracted from $\pi\pi$ scattering in the $I=2$ channel we quote

$$
\begin{array}{llll}
N_f = 2+1+1: & a_0^2 M_\pi = -0.0441(4) & \text{Refs. [20],} & \\
N_f = 2: & a_0^2 M_\pi = -0.04385(47) & \text{Refs. [18],} & (117)
\end{array}
$$

where the errors include both statistical and systematic uncertainties. We remark that our preprocessing procedure[6] symmetrizes the asymmetric errors with a slight adjustment of the central value.

In all cases the references shown are the papers with the contributing results, and we ask the readers to cite those papers when quoting these averages.

5.3 Extraction of SU(3) low-energy constants

5.3.1 New results for individual LO SU(3) LECs

We are unaware of any new paper that determines a large number of LECs in the $SU(3)$ framework (as was done, in the past, by the MILC collaboration). However, there is one paper, χQCD 21 [37], with a new result on two $SU(3)$ LECs at LO. They find $F_0 = 67.8(1.2)(3.2)$ and $\Sigma_0 = 232.6(0.9)(2.7)$ in the 3-flavour chiral limit[7]. They also quote $\Sigma/\Sigma_0 = 1.40(2)(2)$ which we consider ieresting for reasons detailed in Sec. 5.3.4.

These values are listed, together with those of FLAG 19, in Tab. 26. The paper has been discussed and color coded in Sec. 5.2. As they are not published yet, there is no update to the FLAG averages/estimates here.

---

[6]There are two naive procedures to symmetrize an asymmetric systematic error: (i) keep the central value untouched and enlarge the smaller error, (ii) shift the central value by half of the difference between the two original errors and enlarge/shrink both errors by the same amount. Our procedure (iii) is to average the results of (i) and (ii). In other words a result $c(s)\binom{+u}{-\ell}$ with $\ell > u$ is changed into $c + (u-\ell)/4$ with statistical error s and a symmetric systematic error $(u+3\ell)/4$. The case $\ell < u$ is handled accordingly.

[7]We use $\Sigma = \lim_{m_u,m_d \to 0} \Sigma(m_u, m_d, m_s, m_c, ...)$, $\Sigma_0 = \lim_{m_u,m_d,m_s \to 0} \Sigma(m_u, m_d, m_s, m_c, ...)$, and likewise for B, B_0, F and F_0. The quantities Σ, Σ_0, B, B_0 are renormalized at the scale $\mu = 2\,\text{GeV}$.

Collaboration	Ref.	N_f	publication status	chiral extrapolation	cont. extrapolation	finite volume	F_0 [MeV]	F/F_0	B/B_0
JLQCD/TWQCD 10A	[50]	3	A	■	■	■	71(3)(8)		
χQCD 21	[37]	2+1	P	★	★	★	67.8(1.2)(3.2)		
MILC 10	[79]	2+1	C	○	★	★	80.3(2.5)(5.4)		
MILC 09A	[54]	2+1	C	○	★	★	78.3(1.4)(2.9)	*1.104(3)(41)*	*1.21(4)$\binom{+5}{-6}$*
MILC 09	[55]	2+1	A	○	★	★		1.15(5)$\binom{+13}{-03}$	1.15(16)$\binom{+39}{-13}$
PACS-CS 08	[57]	2+1	A	★	■	■	83.8(6.4)	1.078(44)	1.089(15)
RBC/UKQCD 08	[58]	2+1	A	○	■	○	66.1(5.2)	1.229(59)	1.03(05)

Collaboration	Ref.	N_f	publication status	chiral extrapolation	cont. extrapolation	finite volume	renormalization	$\Sigma_0^{1/3}$ [MeV]	Σ/Σ_0
JLQCD/TWQCD 10A	[50]	3	A	■	■	■	★	214(6)(24)	*1.31(13)(52)*
χQCD 21	[37]	2+1	P	★	★	★	★	232.6(0.9)(2.7)	1.40(2)(2)
MILC 09A	[54]	2+1	C	○	★	★	○	245(5)(4)(4)	*1.48(9)(8)(10)*
MILC 09	[55]	2+1	A	○	★	★	○	242(9)$\binom{+05}{-17}$(4)	1.52(17)$\binom{+38}{-15}$
PACS-CS 08	[57]	2+1	A	★	■	■	■	290(15)	1.245(10)
RBC/UKQCD 08	[58]	2+1	A	○	■	○	★		1.55(21)

Table 26: Lattice results for the low-energy constants F_0, B_0 and $\Sigma_0 \equiv F_0^2 B_0$, which specify the effective $SU(3)$ Lagrangian at leading order. The ratios F/F_0, B/B_0, Σ/Σ_0, which compare these with their $SU(2)$ counterparts, indicate the strength of the Zweig-rule violations in these quantities (in the large-N_c limit, they tend to unity). Numbers in slanted fonts are calculated by us, from the information given in the references.

5.3.2   New results for individual NLO SU(3) LECs

There are a number of new results on L_5, for instance in Refs. [35, 112, 113] to be discussed below in the context of πK scattering. This is not so surprising, since Eqns. (101, 102, 103, 104) indicate that the observables $a_0^2 M_\pi$, $a_0^1 M_K$, $a_0^{3/2}\mu_{\pi K}$, $a_0^{1/2}\mu_{\pi K}$ jointly determine the combination $L_{\rm scat}$ and L_5 (both of which are conventionally quoted at the scale $\mu = 770\,{\rm MeV}$). Determining any of these two LECs is afflicted with an extra uncertainty, compared to the four scattering lengths, due to the convergence of the $SU(3)$ chiral series[8]. Therefore we give preference to reviewing the scattering lengths and converting, once they exist, the pertinent FLAG averages into numerical values of $L_{\rm scat}$ and L_5, over collecting values of $L_{\rm scat}$ and L_5 as converted by the individual collaborations.

On the other hand, there is no new result on those LECs at the NLO in the $SU(3)$ expansion which were covered in previous editions of FLAG (L_4, L_6, L_9, L_{10}).

5.3.3   Results for SU(3) linear combinations linked to πK, KK scattering

Since πK, KK scattering were not covered in previous editions of the FLAG report, we list here all works which include such results. Following the example of the section on $\pi\pi$ scattering, where all results were given in the dimensionless variable $a_0^I M_\pi$, we give the results on πK scattering in the form $a_0^I \mu_{\pi K}$, where $\mu_{\pi K}$ is the pertinent reduced mass, and the results on KK scattering are given in the form $a_0^I M_K$. We start with a brief mentioning of all papers we are aware of.

The paper NPLQCD 06B [35] uses asqtad (staggered) sea quarks with $N_f = 2 + 1$ at a single lattice spacing ($a = 0.125$fm with $L \simeq 2.5$fm) with $M_\pi = [290, 350, 490, 600]\,{\rm MeV}$. The domain-wall valence fermions come with quark masses such that the resulting pion masses match the aforementioned Nambu-Goldstone boson masses. After chiral extrapolation they find $a_0^{1/2}\mu_{\pi K} = 0.1346(13)\left(^{+18}_{-122}\right)$ and $a_0^{3/2}\mu_{\pi K} = -0.0448(12)\left(^{+19}_{-45}\right)$, with L_5 pinned down at a value extracted from the analysis of the quark mass dependence of f_K/f_π. The color coding in Tab. 27 is based on $M_{\pi,{\rm min}}({\rm RMS}) = 488\,{\rm MeV}$.

The paper NPLQCD 07B [114] uses asqtad (staggered) sea quarks with $N_f = 2 + 1$ in conjunction with domain-wall valence quarks. They have two lattice spacings ($a = 0.125\,{\rm fm}, 0.09\,{\rm fm}$) with somehat unequal span in quark masses. At $a = 0.125\,{\rm fm}$ they cover $M_\pi \simeq 290, 350, 490, 590\,{\rm MeV}$ with $L \simeq 2.5$fm. At $a = 0.09\,{\rm fm}$ they do not quote $M_\pi[{\rm MeV}]$, but from $aM_\pi = 0.1453$ in Tab.II and $a \simeq 0.09\,{\rm fm}$ one would conclude $M_\pi \simeq 320\,{\rm MeV}$. After chiral extrapolation, they find $a_0^1 M_K = -0.352(16)_{\rm tot}$. The color coding in Tab. 27 is based on $M_{\pi,{\rm min}}({\rm RMS}) = 413\,{\rm MeV}$.

The paper Fu 11A [112] employs one ensemble of $N_f = 2 + 1$ asqtad (staggered) quarks at $a \simeq 0.15\,{\rm fm}$, $m_l/m_s = 0.2$, $m_s \simeq m_s^{\rm phys}$ with $L = 2.5\,{\rm fm}$. It uses six valence pion masses $M_\pi = 334 - 466\,{\rm MeV}$ to study S-wave scattering. It quotes, after chiral extrapolation, $a_0^{1/2}\mu_{\pi K} = 0.1425(29)$ and $a_0^{3/2}\mu_{\pi K} = -0.0394(15)$. The color coding in Tab. 27 is based on $M_{\pi,{\rm min}}({\rm RMS}) = 590\,{\rm MeV}$.

We are also aware of Ref. [115] which is based on a single ensemble of $N_f = 2$ clover quarks. Since it is away from the physical mass point and no extrapolation to the latter is attempted, we feel it would be unfair (or misleading) to quote its results in Tab. 27.

---

[8]One of the issues is whether the convergence in the LECs pertinent to $a_0^1 M_K$, i.e., with two strange quarks involved, is visibly slower than for $a_0^{3/2}\mu_{\pi K}$ and $a_0^{1/2}\mu_{\pi K}$, where only one strange quark appears.

Reference PACS-CS 13 [30] uses five ensembles of $N_f = 2 + 1$ nonpertubative clover fermions with $a = 0.09$fm, $L = 2.9$fm, and $M_\pi = 166, 297, 414, 575, 707$ MeV. They quote, after extrapolation with χPT: $a_0^2 M_\pi = -0.04243(22)(43)$ (see Tab. 25), $a_0^1 M_K = -0.312(17)(31)$, $a_0^{3/2} \mu_{\pi K} = -0.0477(27)(20)$ and $a_0^{1/2} \mu_{\pi K} = 0.150(16)(37)$ (listed in Tab. 27). These figures reflect the final numbers quoted in the Erratum of Ref. [30]. The reason for the change is the mishap reported in footnote 21; fortunately it turns out that it affected the final analysis only very mildly. We thank the collaboration for keeping us up-to-date with all aspects of the revision. Since there are no FLAG averages for scattering lengths for $N_f = 2 + 1$, these small changes have no impact on the quoted FLAG averages.

The paper HS 14A [116] is based on $N_f = 2+1$ anisotropic clover fermions at $a_s \simeq 0.12$ fm, $a_t \simeq 0.035$ fm, with $M_\pi = 391$ MeV in $\{16^3, 20^3, 24^3\} \times 128$ boxes, i.e. with $L = 1.9, 2.4, 2.9$ fm. These parameters yield $M_K = 549$ MeV thus $\mu_{\pi K} = 228$ MeV. They quote various resonance parameters and, in the S-wave $I = 3/2$ channel, $a_0^{3/2} M_\pi = -0.278(15)$ which we convert to $a_0^{3/2} \mu_{\pi K} = -0.161(9)$ at the given M_π. Since this work does not extrapolate to M_π^{phys}, we stay away from color coding.

The paper ETM 17G [117] uses $N_f = 2 + 1 + 1$ twisted mass fermions at three lattice spacings, $a = 0.089, 0.082, 0.062$ fm, with up to five $M_\pi = 230 - 450$ MeV, and $L(M_{\pi,\min}) \simeq 2.8$ fm. In the $I = 1$ channel they find $a_0^1 M_K = -0.385(16)\binom{+0}{-12}\binom{+0}{-5}(4)$. We take the liberty to combine the various non-statistical errors in quadrature, using $a_0^1 M_K = -0.385(16)\binom{+4}{-14}$ as quoted in Tab. 27.

Reference [118] by R. Brett *et al.* uses one ensemble of $N_f = 2 + 1$ anisotropic clover fermions with $a_s = 0.115$ fm, $M_\pi = 233$ MeV, in a $32^3 \times 256$ box, hence $L = 3.7$fm. These parameters yield $M_K = 494$ MeV and thus $\mu_{\pi K} = 158$ MeV. Their result for $I = 1/2$ S-wave scattering reads $a_0^{1/2} M_\pi = -0.353(25)$, or $a_0^{1/2} \mu_{\pi K} = -0.240(17)$ in our notation. Since this work does not extrapolate to M_π^{phys}, we stay away from color coding.

The paper ETM 18B [119] uses $N_f = 2 + 1 + 1$ twisted mass fermions at three lattice spacings, $a = 0.089, 0.082, 0.062$ fm, with up to five pion masses $M_\pi = 230 - 450$ MeV and up to two volumes. From the tables, one finds $M_{\pi,\min} = 276, 302, 311$ MeV at the three lattice spacings. They find, after chiral extrapolation, $a_0^{1/2} \mu_{\pi K} = 0.127(2)_{\text{tot}}$ and $a_0^{3/2} \mu_{\pi K} = -0.0463(17)_{\text{tot}}$ as quoted in Tab. 27.

An overview of all scattering lengths with at least one kaon involved is shown in Fig. 19. As usual we refrain from displaying data with statistical error only.

In passing, we note that there is an additional paper by Z. Fu, Ref. [113], which deals with $K\bar{K}$ scattering. It employs one ensemble of $N_f = 2 + 1$ asqtad (staggered) quarks at $a \simeq 0.15$ fm, $m_l/m_s = 0.2$, $m_s \simeq m_s^{\text{phys}}$ with $L = 2.5$ fm together with six valence pion masses $M_\pi = 334 - 466$ MeV. Extrapolating to the physical point, the result for $K\bar{K}$ scattering in the $I = 1$ state is $a_0^1 M_K = 0.211(33)$. Hence the interaction for $K\bar{K}$ in the S-wave $I = 1$ state is found to be attractive, in agreement with LO χPT.

In summary, for the quantities $a_0^{1/2} \mu_{\pi K}$, $a_0^{3/2} \mu_{\pi K}$ and $a_0^1 M_K$ Refs. [117, 119] are the only sources without red tags. Since they appeared in refereed journals and no other works qualify, we take the results quoted in the top two lines of Tab. 27 as the current FLAG averages. For the reader's convenience we list them at the end of Sec. 5.3.5.

Last but not least we like to remind the reader that KK scattering might be outside the validity of $SU(3)$ χPT, since it involves a scale around $2M_K \simeq 1$ GeV. However, our review focuses on the scattering length $a_0^1 M_K$, where this issue does not feature prominently. But

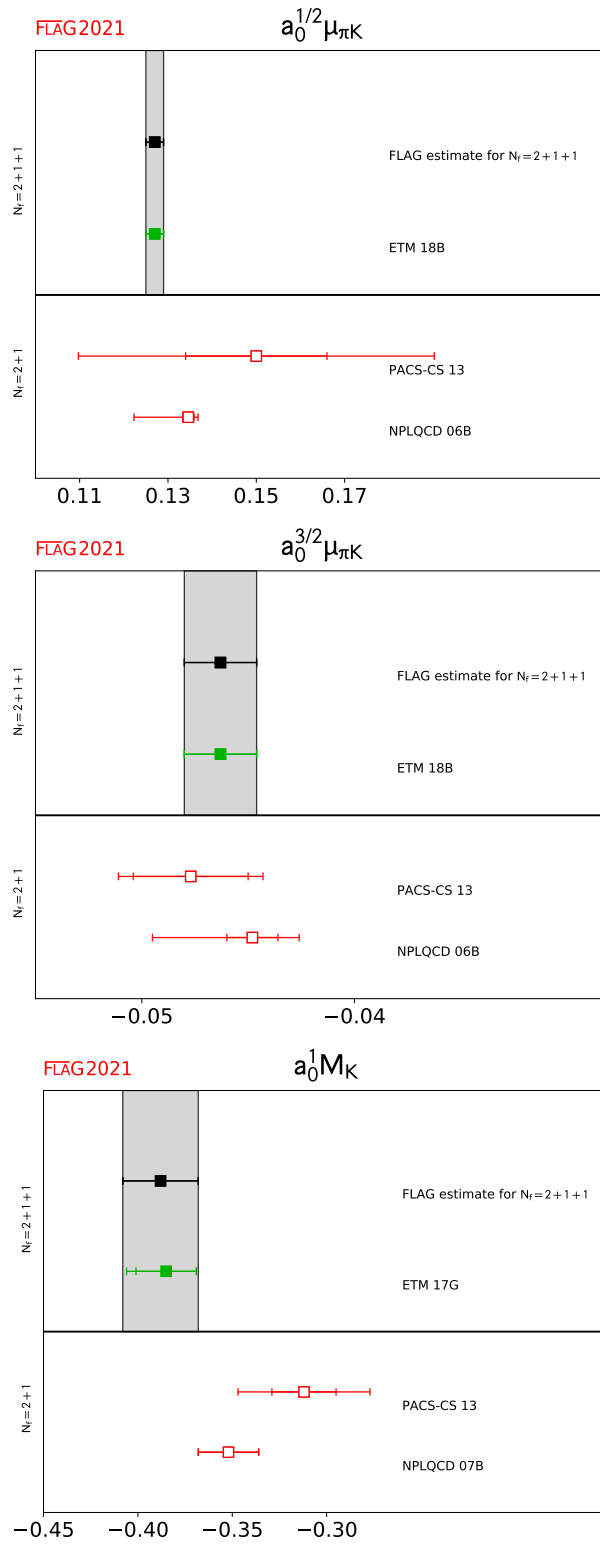Figure 19: Summary of the πK scattering lengths $a_0^{1/2}\mu_{\pi K}$ (top), $a_0^{3/2}\mu_{\pi K}$ (middle) and of the KK scattering length $a_0^1 M_K$ (bottom). Results in Tab. 27 with statistical error only are not shown.

Collaboration	Ref.	N_f	publication status	chiral extrapolation	cont. extrapolation	finite volume	$a_0^{1/2}\mu_{\pi K}$	$a_0^{3/2}\mu_{\pi K}$	$a_0^1 M_K$
ETM 18B	[119]	2+1+1	A	○	★	○	$0.127(2)_{\text{tot}}$	$-0.0463(17)_{\text{tot}}$	
ETM 17G	[117]	2+1+1	A	○	★	○			$-0.385(16)\binom{+4}{-14}$
PACS-CS 13	[30]	2+1	A	★	■	■	$0.150(16)(37)$	$-0.0477(27)(20)$	$-0.312(17)(31)$
Fu 11A	[112]	2+1	A	■	■	★	$0.1425(29)$	$-0.0394(15)$	
NPLQCD 07B	[114]	2+1	A	■	○	○			$-0.352(16)_{\text{tot}}$
NPLQCD 06B	[35]	2+1	A	■	■	★	$0.1346(13)\binom{+18}{-122}$	$-0.0448(12)\binom{+19}{-45}$	

Table 27: Summary of πK scattering data in the $I = \frac{1}{2}, \frac{3}{2}$ channels, and of KK scattering with $I = 1$. Some of the results have been adapted to our sign convention.

it is a key topic in the subsequent conversion of such a scattering length to the low-energy constants L_i. We hope that forthcoming high-quality data will allow a future edition of FLAG to address this topic.

5.3.4 Implication on Zweig rule violations

Let us spend a minute to explain why we consider the result on Σ/Σ_0 of χQCD 21 [37] particularly interesting. The reason is linked to the question of how close real-world QCD with $N_c = 3$ is to the large-N_c limit of 't Hooft (see also Ref. [120]). In the large-N_c limit the Zweig rule becomes exact, and the NLO LECs L_4 and L_6 tend to zero. As discussed in FLAG 19, the available lattice data are consistent with the view that these two couplings approximately satisfy the Zweig rule. Also the ratios F/F_0, B/B_0 and Σ/Σ_0 (note that they are linearly dependent, since $\Sigma = BF^2$ and $\Sigma_0 = B_0 F_0^2$) test the validity of this rule.

The available data seem to confirm the paramagnetic inequalities of Ref. [121], which require $\Sigma/\Sigma_0 > 1$ and $F/F_0 > 1$. There is much less information concerning B/B_0, and this is the point where the new result of χQCD 21 [37] comes in handy. Let us assume, for the sake of an argument, $F/F_0 = 1.15(5)(5)$. Together with $\Sigma/\Sigma_0 = 1.40(2)(2)$ [37], this would imply $B/B_0 = 1.06(9)(9)$. This numerical example illustrates how much precision is lost in forming the ratio $(\Sigma/\Sigma_0)/(F/F_0)^2$; with these numbers it would not be clear whether $B/B_0 > 1$. Therefore we plead with all collaborations to calculate the numbers F/F_0, B/B_0 and Σ/Σ_0 in their analysis framework to take advantage of correlations.

5.3.5 LO and NLO $SU(3)$ estimates

For each of the $SU(3)$ LO and NLO LECs discussed in the 2019 FLAG review [3] exactly one paper contributed and hence constituted the FLAG average. The present status is that this situation is unchanged. For the convenience of the reader, we list the results here but refer to the 2019 FLAG review for the details and explanations.

The LO LECs in the $SU(3)$ chiral limit $(m_u, m_d, m_s \to 0)$ are denoted by a subscript 0 to distinguish them from their $SU(2)$ chiral limit counterparts. The parameters Σ_0, B_0 are

in the $\overline{\text{MS}}$ scheme at the renormalization scale $\mu = 2\,\text{GeV}$. We quote

$$
\begin{array}{llll}
N_f = 2 + 1: & \Sigma_0^{1/3} = 245(8)\,\text{MeV} & \text{Ref. [54]}, & (118) \\
N_f = 2 + 1: & \Sigma/\Sigma_0 = 1.48(16) & \text{Ref. [54]}, & (119) \\
N_f = 2 + 1: & F_0 = 80.3(6.0)\,\text{MeV} & \text{Ref. [79]}, & (120) \\
N_f = 2 + 1: & F/F_0 = 1.104(41) & \text{Ref. [54]}, & (121) \\
N_f = 2 + 1: & B/B_0 = 1.21(7) & \text{Ref. [54]}, & (122)
\end{array}
$$

where the errors include both statistical and systematic uncertainties. The references shown are the papers from which the results are taken.

For $SU(3)$ NLO LECs we display the results for individual low-energy constants

$$
\begin{array}{llll}
N_f = 2 + 1 + 1: & L_4 = +0.09(34) \times 10^{-3} & \text{Ref. [122]}, & \\
N_f = 2 + 1: & L_4 = -0.02(56) \times 10^{-3} & \text{Ref. [79]}, & (123) \\
N_f = 2 + 1 + 1: & L_5 = +1.19(25) \times 10^{-3} & \text{Ref. [122]}, & \\
N_f = 2 + 1: & L_5 = +0.95(41) \times 10^{-3} & \text{Ref. [79]}, & (124) \\
N_f = 2 + 1 + 1: & L_6 = +0.16(20) \times 10^{-3} & \text{Ref. [122]}, & \\
N_f = 2 + 1: & L_6 = +0.01(34) \times 10^{-3} & \text{Ref. [79]}, & (125) \\
N_f = 2 + 1 + 1: & L_8 = +0.55(15) \times 10^{-3} & \text{Ref. [122]}, & \\
N_f = 2 + 1: & L_8 = +0.43(28) \times 10^{-3} & \text{Ref. [79]}, & (126)
\end{array}
$$

at the chiral scale $\mu = 770\,\text{MeV}$, where again all errors quoted are total errors. For details of the symmetrization of asymmetric error bars see footnote 23.

For the scattering lengths involving at least one kaon

$$
\begin{array}{llll}
N_f = 2 + 1 + 1: & a_0^{1/2}\mu_{\pi K} = 0.127(2) & \text{Ref. [119]}, & (127) \\
N_f = 2 + 1 + 1: & a_0^{3/2}\mu_{\pi K} = -0.0463(17) & \text{Ref. [119]}, & (128) \\
N_f = 2 + 1 + 1: & a_0^1 M_K = -0.388(20) & \text{Ref. [117]}, & (129)
\end{array}
$$

represent the FLAG estimates with all errors added in quadrature. For details of the symmetrization of asymmetric error bars see footnote 23. Throughout we ask the reader to cite the original references when using these values.

References

[1] J. Gasser and H. Leutwyler, *Chiral perturbation theory to one loop*, *Ann. Phys.* **158** (1984) 142.

[2] J. Gasser and H. Leutwyler, *Chiral perturbation theory: expansions in the mass of the strange quark*, *Nucl. Phys.* **B250** (1985) 465.

[3] [FLAG 19] S. Aoki et al., *FLAG Review 2019: Flavour Lattice Averaging Group (FLAG)*, *Eur. Phys. J. C* **80** (2020) 113 [1902.08191].

[4] S. Weinberg, *Pion scattering lengths*, *Phys. Rev. Lett.* **17** (1966) 616.

[5] J. Gasser and H. Leutwyler, *Low-Energy Theorems as Precision Tests of QCD*, *Phys. Lett.* **125B** (1983) 325.

[6] J. Bijnens, G. Colangelo, G. Ecker, J. Gasser and M.E. Sainio, *Elastic pi pi scattering to two loops*, *Phys. Lett.* **B374** (1996) 210 [`hep-ph/9511397`].

[7] G. Colangelo, J. Gasser and H. Leutwyler, $\pi\pi$ *scattering*, *Nucl. Phys.* **B603** (2001) 125 [`hep-ph/0103088`].

[8] J. Nebreda and J.R. Pelaez., *Strange and non-strange quark mass dependence of elastic light resonances from SU(3) Unitarized Chiral Perturbation Theory to one loop*, *Phys. Rev.* **D81** (2010) 054035 [`1001.5237`].

[9] L. Maiani and M. Testa, *Final state interactions from Euclidean correlation functions*, *Phys. Lett.* **B245** (1990) 585.

[10] M. Lüscher, *Volume Dependence of the Energy Spectrum in Massive Quantum Field Theories. 1. Stable Particle States*, *Commun. Math. Phys.* **104** (1986) 177.

[11] M. Lüscher, *Volume Dependence of the Energy Spectrum in Massive Quantum Field Theories. 2. Scattering States*, *Commun. Math. Phys.* **105** (1986) 153.

[12] M. Lüscher, *Two particle states on a torus and their relation to the scattering matrix*, *Nucl. Phys.* **B354** (1991) 531.

[13] M. Lüscher, *Signatures of unstable particles in finite volume*, *Nucl. Phys.* **B364** (1991) 237.

[14] S.M. Roy, *Exact integral equation for pion pion scattering involving only physical region partial waves*, *Phys. Lett.* **36B** (1971) 353.

[15] B. Ananthanarayan, G. Colangelo, J. Gasser and H. Leutwyler, *Roy equation analysis of pi pi scattering*, *Phys. Rept.* **353** (2001) 207 [`hep-ph/0005297`].

[16] I. Caprini, G. Colangelo and H. Leutwyler, *Regge analysis of the pi pi scattering amplitude*, *Eur. Phys. J.* **C72** (2012) 1860 [`1111.7160`].

[17] [NPLQCD 07] S. R. Beane et al., *Precise determination of the I=2 $\pi\pi$ scattering length from mixed-action lattice QCD*, *Phys. Rev.* **D77** (2008) 014505 [`0706.3026`].

[18] [ETM 09G] X. Feng, K. Jansen and D.B. Renner, *The pi+ pi+ scattering length from maximally twisted mass lattice QCD*, *Phys. Lett.* **B684** (2010) 268 [`0909.3255`].

[19] Z. Fu, *Lattice QCD study of the s-wave $\pi\pi$ scattering lengths in the I=0 and 2 channels*, *Phys. Rev.* **D87** (2013) 074501 [`1303.0517`].

[20] [ETM 15E] C. Helmes, C. Jost, B. Knippschild, C. Liu, J. Liu, L. Liu et al., *Hadron-hadron interactions from $N_f = 2 + 1 + 1$ lattice QCD: isospin-2 π-π scattering length*, *JHEP* **09** (2015) 109 [`1506.00408`].

[21] [ETM 16C] L. Liu et al., *Isospin-0 $\pi\pi$ s-wave scattering length from twisted mass lattice QCD*, *Phys. Rev.* **D96** (2017) 054516 [`1612.02061`].

[22] PARTICLE DATA GROUP collaboration, *Review of Particle Physics*, *Chin. Phys.* **C38** (2014) 090001 and 2015 update.

[23] J.-W. Chen, D. O'Connell, R.S. Van de Water and A. Walker-Loud, *Ginsparg-Wilson pions scattering on a staggered sea*, *Phys. Rev.* **D73** (2006) 074510 [`hep-lat/0510024`].

[24] M.I. Buchoff, *Isotropic and Anisotropic Lattice Spacing Corrections for I=2 pi-pi Scattering from Effective Field Theory*, *Phys. Rev.* **D77** (2008) 114502 [`0802.2931`].

[25] S. Aoki, O. Bar and B. Biedermann, *Pion scattering in Wilson chiral perturbation theory*, *Phys. Rev.* **D78** (2008) 114501 [`0806.4863`].

[26] N.R. Acharya, F.-K. Guo, U.-G. Meissner and C.-Y. Seng, *Connected and disconnected contractions in pion-pion scattering*, *Nucl. Phys.* **B922** (2017) 480 [`1704.06754`].

[27] G. Burdman and J.F. Donoghue, *Union of chiral and heavy quark symmetries*, *Phys. Lett. B* **280** (1992) 287.

[28] M.B. Wise, *Chiral perturbation theory for hadrons containing a heavy quark*, *Phys. Rev. D* **45** (1992) R2188.

[29] T.-M. Yan, H.-Y. Cheng, C.-Y. Cheung, G.-L. Lin, Y.C. Lin and H.-L. Yu, *Heavy quark symmetry and chiral dynamics*, *Phys. Rev. D* **46** (1992) 1148 [Erratum: Phys.Rev.D 55, 5851 (1997)].

[30] [PACS-CS 13] K. Sasaki, N. Ishizuka, M. Oka and T. Yamazaki, *Scattering lengths for two pseudoscalar meson systems*, *Phys. Rev.* **D89** (2014) 054502 [`1311.7226`].

[31] V. Bernard, N. Kaiser and U.G. Meissner, *pi K scattering in chiral perturbation theory to one loop*, *Nucl. Phys. B* **357** (1991) 129.

[32] V. Bernard, N. Kaiser and U.G. Meissner, *Threshold parameters of pi K scattering in QCD*, *Phys. Rev. D* **43** (1991) 2757.

[33] B. Kubis and U.-G. Meissner, *Isospin violation in low-energy charged pion kaon scattering*, *Phys. Lett. B* **529** (2002) 69 [`hep-ph/0112154`].

[34] J.-W. Chen, D. O'Connell and A. Walker-Loud, *Two meson systems with Ginsparg-Wilson valence quarks*, *Phys. Rev.* **D75** (2007) 054501 [`hep-lat/0611003`].

[35] [NPLQCD 06B] S. R. Beane, P.F. Bedaque, T.C. Luu, K. Orginos, E. Pallante, A. Parreno et al., *pi K scattering in full QCD with domain-wall valence quarks*, *Phys. Rev. D* **74** (2006) 114503 [`hep-lat/0607036`].

[36] [ETM 20A] M. Fischer, B. Kostrzewa, M. Mai, M. Petschlies, F. Pittler, M. Ueding et al., *The ρ-resonance with physical pion mass from $N_f = 2$ lattice QCD*, *Phys. Lett. B* **819** (2021) 136449 [`2006.13805`].

[37] [χQCD 21] J. Liang, A. Alexandru, Y.-J. Bi, T. Draper, K.-F. Liu and Y.-B. Yang, *Detecting flavors of vacuum from the Dirac operator spectrum*, [`2102.05380`].

[38] [ETM 21] C. Alexandrou et al., *Ratio of kaon and pion leptonic decay constants with* $N_f = 2 + 1 + 1$ *Wilson-clover twisted-mass fermions*, *Phys. Rev. D* **104** (2021) 074520 [2104.06747].

[39] S. Dürr, *Validity of ChPT - is* $M_\pi = 135$ *MeV small enough?*, *PoS* **LATTICE2014** (2015) 006 [1412.6434].

[40] [ETM 21A] C. Alexandrou et al., *Quark masses using twisted mass fermion gauge ensembles*, *Phys. Rev. D* **104** (2021) 074515 [2104.13408].

[41] C. Wang, Y. Bi, H. Cai, Y. Chen, M. Gong and Z. Liu, *Quark chiral condensate from the overlap quark propagator*, *Chin. Phys. C* **41** (2017) 053102 [1612.04579].

[42] [ETMC 17E] C. Alexandrou, A. Athenodorou, K. Cichy, M. Constantinou, D.P. Horkel, K. Jansen et al., *Topological susceptibility from twisted mass fermions using spectral projectors and the gradient flow*, *Phys. Rev.* **D97** (2018) 074503 [1709.06596].

[43] [ETM 13] K. Cichy, E. Garcia-Ramos and K. Jansen, *Chiral condensate from the twisted mass Dirac operator spectrum*, *JHEP* **1310** (2013) 175 [1303.1954].

[44] [JLQCD 17A] S. Aoki, G. Cossu, H. Fukaya, S. Hashimoto and T. Kaneko, *Topological susceptibility of QCD with dynamical Möbius domain wall fermions*, *PTEP* **2018** (2018) 043B07 [1705.10906].

[45] [JLQCD 16B] G. Cossu, H. Fukaya, S. Hashimoto, T. Kaneko and J.-I. Noaki, *Stochastic calculation of the Dirac spectrum on the lattice and a determination of chiral condensate in 2+1-flavor QCD*, *PTEP* **2016** (2016) 093B06 [1607.01099].

[46] [RBC/UKQCD 15E] P. A. Boyle et al., *Low energy constants of SU(2) partially quenched chiral perturbation theory from* $N_f = 2 + 1$ *domain wall QCD*, *Phys. Rev.* **D93** (2016) 054502 [1511.01950].

[47] [RBC/UKQCD 14B] T. Blum et al., *Domain wall QCD with physical quark masses*, *Phys. Rev.* **D93** (2016) 074505 [1411.7017].

[48] [BMW 13] S. Dürr, Z. Fodor, C. Hoelbling, S. Krieg, T. Kurth et al., *Lattice QCD at the physical point meets SU(2) chiral perturbation theory*, *Phys. Rev.* **D90** (2014) 114504 [1310.3626].

[49] S. Borsanyi, S. Dürr, Z. Fodor, S. Krieg, A. Schäfer et al., *SU(2) chiral perturbation theory low-energy constants from 2+1 flavor staggered lattice simulations*, *Phys.Rev.* **D88** (2013) 014513 [1205.0788].

[50] [JLQCD/TWQCD 10A] H. Fukaya et al., *Determination of the chiral condensate from QCD Dirac spectrum on the lattice*, *Phys. Rev.* **D83** (2011) 074501 [1012.4052].

[51] [MILC 10A] A. Bazavov et al., *Staggered chiral perturbation theory in the two-flavor case and SU(2) analysis of the MILC data*, *PoS* **LAT2010** (2010) 083 [1011.1792].

[52] [RBC/UKQCD 10A] Y. Aoki et al., *Continuum limit physics from 2+1 flavor domain wall QCD*, *Phys.Rev.* **D83** (2011) 074508 [1011.0892].

[53] [JLQCD 09] H. Fukaya et al., *Determination of the chiral condensate from 2+1-flavor lattice QCD*, *Phys. Rev. Lett.* **104** (2010) 122002 [0911.5555].

[54] [MILC 09A] A. Bazavov et al., *MILC results for light pseudoscalars*, *PoS* **CD09** (2009) 007 [0910.2966].

[55] [MILC 09] A. Bazavov et al., *Full nonperturbative QCD simulations with 2+1 flavors of improved staggered quarks*, *Rev. Mod. Phys.* **82** (2010) 1349 [0903.3598].

[56] [TWQCD 08] T.-W. Chiu, T.-H. Hsieh and P.-K. Tseng, *Topological susceptibility in 2+1 flavors lattice QCD with domain-wall fermions*, *Phys. Lett.* **B671** (2009) 135 [0810.3406].

[57] [PACS-CS 08] S. Aoki et al., *2+1 flavor lattice QCD toward the physical point*, *Phys. Rev.* **D79** (2009) 034503 [0807.1661].

[58] [RBC/UKQCD 08] C. Allton et al., *Physical results from 2+1 flavor domain wall QCD and SU(2) chiral perturbation theory*, *Phys. Rev.* **D78** (2008) 114509 [0804.0473].

[59] G.P. Engel, L. Giusti, S. Lottini and R. Sommer, *Spectral density of the Dirac operator in two-flavor QCD*, *Phys. Rev.* **D91** (2015) 054505 [1411.6386].

[60] B. B. Brandt, A. Jüttner and H. Wittig, *The pion vector form factor from lattice QCD and NNLO chiral perturbation theory*, *JHEP* **1311** (2013) 034 [1306.2916].

[61] [ETM 12] F. Burger, V. Lubicz, M. Muller-Preussker, S. Simula and C. Urbach, *Quark mass and chiral condensate from the Wilson twisted mass lattice quark propagator*, *Phys.Rev.* **D87** (2013) 034514 [1210.0838].

[62] F. Bernardoni, N. Garron, P. Hernandez, S. Necco and C. Pena, *Light quark correlators in a mixed-action setup*, *PoS* **LAT2011** (2011) 109 [1110.0922].

[63] [TWQCD 11] T.-W. Chiu, T.-H. Hsieh and Y.-Y. Mao, *Pseudoscalar meson in two flavors QCD with the optimal domain-wall fermion*, *Phys.Lett.* **B717** (2012) 420 [1109.3675].

[64] [TWQCD 11A] T.-W. Chiu, T.H. Hsieh and Y.Y. Mao, *Topological susceptibility in two flavors lattice QCD with the optimal domain-wall fermion*, *Phys.Lett.* **B702** (2011) 131 [1105.4414].

[65] F. Bernardoni, P. Hernandez, N. Garron, S. Necco and C. Pena, *Probing the chiral regime of $N_f = 2$ QCD with mixed actions*, *Phys. Rev.* **D83** (2011) 054503 [1008.1870].

[66] [ETM 09C] R. Baron et al., *Light meson physics from maximally twisted mass lattice QCD*, *JHEP* **08** (2010) 097 [0911.5061].

[67] [ETM 08] R. Frezzotti, V. Lubicz and S. Simula, *Electromagnetic form factor of the pion from twisted-mass lattice QCD at $N_f = 2$*, *Phys. Rev.* **D79** (2009) 074506 [0812.4042].

[68] [CERN 08] L. Giusti and M. Lüscher, *Chiral symmetry breaking and the Banks–Casher relation in lattice QCD with Wilson quarks*, *JHEP* **03** (2009) 013 [0812.3638].

[69] A. Hasenfratz, R. Hoffmann and S. Schaefer, *Low energy chiral constants from ε-regime simulations with improved Wilson fermions*, *Phys. Rev.* **D78** (2008) 054511 [0806.4586].

[70] [JLQCD/TWQCD 08A] J. Noaki et al., *Convergence of the chiral expansion in two-flavor lattice QCD*, *Phys. Rev. Lett.* **101** (2008) 202004 [0806.0894].

[71] [JLQCD/TWQCD 07] H. Fukaya et al., *Lattice study of meson correlators in the ε-regime of two-flavor QCD*, *Phys. Rev.* **D77** (2008) 074503 [0711.4965].

[72] [JLQCD/TWQCD 07A] S. Aoki et al., *Topological susceptibility in two-flavor lattice QCD with exact chiral symmetry*, *Phys. Lett.* **B665** (2008) 294 [0710.1130].

[73] Y. Aoki, S. Borsanyi, S. Dürr, Z. Fodor, S.D. Katz, S. Krieg et al., *The QCD transition temperature: results with physical masses in the continuum limit II.*, *JHEP* **06** (2009) 088 [0903.4155].

[74] [HotQCD 14] A. Bazavov et al., *Equation of state in (2+1)-flavor QCD*, *Phys.Rev.* **D90** (2014) 094503 [1407.6387].

[75] [ETM 15A] A. Abdel-Rehim et al., *Simulating QCD at the physical point with $N_f = 2$ Wilson twisted mass fermions at maximal twist*, *Phys. Rev.* **D95** (2015) 094515 [1507.05068].

[76] [ETM 11] R. Baron et al., *Light hadrons from $N_f = 2 + 1 + 1$ dynamical twisted mass fermions*, *PoS* **LAT2010** (2010) 123 [1101.0518].

[77] [ETM 10] R. Baron et al., *Light hadrons from lattice QCD with light (u,d), strange and charm dynamical quarks*, *JHEP* **1006** (2010) 111 [1004.5284].

[78] [NPLQCD 11] S. R. Beane, W. Detmold, P. Junnarkar, T. Luu, K. Orginos et al., *SU(2) low-energy constants from mixed-action lattice QCD*, *Phys.Rev.* **D86** (2012) 094509 [1108.1380].

[79] [MILC 10] A. Bazavov et al., *Results for light pseudoscalar mesons*, *PoS* **LAT2010** (2010) 074 [1012.0868].

[80] [QCDSF 13] R. Horsley, Y. Nakamura, A. Nobile, P. Rakow, G. Schierholz et al., *Nucleon axial charge and pion decay constant from two-flavor lattice QCD*, *Phys. Lett.* **B732** (2014) 41 [1302.2233].

[81] G. Colangelo and S. Dürr, *The pion mass in finite volume*, *Eur. Phys. J.* **C33** (2004) 543 [hep-lat/0311023].

[82] [RBC/UKQCD 12] R. Arthur et al., *Domain wall QCD with near-physical pions*, *Phys.Rev.* **D87** (2013) 094514 [1208.4412].

[83] V. Gülpers, G. von Hippel and H. Wittig, *The scalar radius of the pion from lattice QCD in the continuum limit*, *Eur. Phys. J.* **A51** (2015) 158 [1507.01749].

[84] V. Gülpers, G. von Hippel and H. Wittig, *The scalar pion form factor in two-flavor lattice QCD*, *Phys. Rev.* **D89** (2014) 094503 [1309.2104].

[85] [JLQCD/TWQCD 09] S. Aoki et al., *Pion form factors from two-flavor lattice QCD with exact chiral symmetry*, *Phys. Rev.* **D80** (2009) 034508 [0905.2465].

[86] [CERN-TOV 06] L. Del Debbio, L. Giusti, M. Lüscher, R. Petronzio and N. Tantalo, *QCD with light Wilson quarks on fine lattices (I): first experiences and physics results*, *JHEP* **02** (2007) 056 [hep-lat/0610059].

[87] [HPQCD 15B] J. Koponen, F. Bursa, C.T.H. Davies, R.J. Dowdall and G.P. Lepage, *The Size of the Pion from Full Lattice QCD with Physical u, d, s and c Quarks*, *Phys. Rev.* **D93** (2016) 054503 [1511.07382].

[88] X. Gao, N. Karthik, S. Mukherjee, P. Petreczky, S. Syritsyn and Y. Zhao, *Pion form factor and charge radius from Lattice QCD at physical point*, *Phys. Rev. D* **104** (2021) 114515 [2102.06047].

[89] [χQCD 20] G. Wang, J. Liang, T. Draper, K.-F. Liu and Y.-B. Yang, *Lattice Calculation of Pion Form Factor with Overlap Fermions*, *Phys. Rev. D* **104** (2021) 074502 [2006.05431].

[90] X. Feng, Y. Fu and L.-C. Jin, *Lattice QCD calculation of the pion charge radius using a model-independent method*, *Phys. Rev. D* **101** (2020) 051502 [1911.04064].

[91] [JLQCD 15A] S. Aoki, G. Cossu, X. Feng, S. Hashimoto, T. Kaneko, J. Noaki et al., *Light meson electromagnetic form factors from three-flavor lattice QCD with exact chiral symmetry*, *Phys. Rev.* **D93** (2016) 034504 [1510.06470].

[92] [JLQCD 14] H. Fukaya, S. Aoki, S. Hashimoto, T. Kaneko, H. Matsufuru and J. Noaki, *Computation of the electromagnetic pion form factor from lattice QCD in the ϵ regime*, *Phys. Rev.* **D90** (2014) 034506 [1405.4077].

[93] [PACS-CS 11A] O. H. Nguyen, K.-I. Ishikawa, A. Ukawa and N. Ukita, *Electromagnetic form factor of pion from $N_f = 2 + 1$ dynamical flavor QCD*, *JHEP* **04** (2011) 122 [1102.3652].

[94] [RBC/UKQCD 08A] P. A. Boyle et al., *The pion's electromagnetic form factor at small momentum transfer in full lattice QCD*, *JHEP* **07** (2008) 112 [0804.3971].

[95] [LHP 04] F. D. R. Bonnet, R.G. Edwards, G.T. Fleming, R. Lewis and D.G. Richards, *Lattice computations of the pion form factor*, *Phys. Rev.* **D72** (2005) 054506 [hep-lat/0411028].

[96] [ETM 17F] C. Alexandrou et al., *Pion vector form factor from lattice QCD at the physical point*, *Phys. Rev.* **D97** (2018) 014508 [1710.10401].

[97] [QCDSF/UKQCD 06A] D. Brömmel et al., *The pion form factor from lattice QCD with two dynamical flavours*, *Eur. Phys. J.* **C51** (2007) 335 [hep-lat/0608021].

[98] J. Bijnens, G. Colangelo and P. Talavera, *The vector and scalar form factors of the pion to two loops*, *JHEP* **05** (1998) 014 [hep-ph/9805389].

[99] S.R. Amendolia et al., *A measurement of the space-like pion electromagnetic form factor*, *Nucl. Phys.* **B277** (1986) 168.

[100] B. Hörz and A. Hanlon, *Two- and three-pion finite-volume spectra at maximal isospin from lattice QCD*, *Phys. Rev. Lett.* **123** (2019) 142002 [1905.04277].

[101] J. Bulava, B. Fahy, B. Horz, K.J. Juge, C. Morningstar and C.H. Wong, $I = 1$ *and* $I = 2$ $\pi - \pi$ *scattering phase shifts from* $N_\mathrm{f} = 2 + 1$ *lattice QCD*, *Nucl. Phys.* **B910** (2016) 842 [1604.05593].

[102] T.D. Blanton, F. Romero-López and S.R. Sharpe, $I = 3$ *Three-Pion Scattering Amplitude from Lattice QCD*, *Phys. Rev. Lett.* **124** (2020) 032001 [1909.02973].

[103] C. Culver, M. Mai, A. Alexandru, M. Döring and F.X. Lee, *Pion scattering in the isospin* $I = 2$ *channel from elongated lattices*, *Phys. Rev. D* **100** (2019) 034509 [1905.10202].

[104] M. Mai, C. Culver, A. Alexandru, M. Döring and F.X. Lee, *Cross-channel study of pion scattering from lattice QCD*, *Phys. Rev. D* **100** (2019) 114514 [1908.01847].

[105] [ETM 20B] M. Fischer, B. Kostrzewa, L. Liu, F. Romero-López, M. Ueding and C. Urbach, *Scattering of two and three physical pions at maximal isospin from lattice QCD*, *Eur. Phys. J. C* **81** (2021) 436 [2008.03035].

[106] Z. Fu and X. Chen, $I = 0$ $\pi\pi$ *s-wave scattering length from lattice QCD*, *Phys. Rev.* **D98** (2018) 014514 [1712.02219].

[107] Z. Fu, *Lattice QCD calculation of* $\pi\pi$ *scattering length*, *Commun. Theor. Phys.* **57** (2012) 78 [1110.3918].

[108] [NPLQCD 11A] S. R. Beane, E. Chang, W. Detmold, H.W. Lin, T.C. Luu, K. Orginos et al., *The I=2 pipi S-wave Scattering Phase Shift from Lattice QCD*, *Phys. Rev.* **D85** (2012) 034505 [1107.5023].

[109] [NPLQCD 05] S. R. Beane, P.F. Bedaque, K. Orginos and M.J. Savage, $I = 2$ *pi-pi scattering from fully-dynamical mixed-action lattice QCD*, *Phys. Rev.* **D73** (2006) 054503 [hep-lat/0506013].

[110] T. Yagi, S. Hashimoto, O. Morimatsu and M. Ohtani, *I=2* π*-*π *scattering length with dynamical overlap fermion*, 1108.2970.

[111] [CP-PACS 04] T. Yamazaki et al., $I = 2$ *pi pi scattering phase shift with two flavors of* $O(a)$ *improved dynamical quarks*, *Phys. Rev.* **D70** (2004) 074513 [hep-lat/0402025].

[112] Z. Fu, *Lattice study on* πK *scattering with moving wall source*, *Phys. Rev. D* **85** (2012) 074501 [1110.1422].

[113] Z. Fu, *Preliminary lattice study of the I=1* $K\bar{K}$ *scattering length*, *Eur. Phys. J.* **72** (2012) 2159 [1201.3708].

[114] [NPLQCD 07B] S. R. Beane et al., *The K+K+ scattering length from lattice QCD*, *Phys. Rev.* **D77** (2008) 094507 [0709.1169].

[115] C.B. Lang, L. Leskovec, D. Mohler and S. Prelovsek, *K pi scattering for isospin 1/2 and 3/2 in lattice QCD*, *Phys. Rev. D* **86** (2012) 054508 [1207.3204].

[116] D.J. Wilson, J.J. Dudek, R.G. Edwards and C.E. Thomas, *Resonances in coupled $\pi K, \eta K$ scattering from lattice QCD*, *Phys. Rev. D* **91** (2015) 054008 [1411.2004].

[117] [ETM 17G] C. Helmes, C. Jost, B. Knippschild, B. Kostrzewa, L. Liu, C. Urbach et al., *Hadron-Hadron Interactions from $N_f = 2+1+1$ lattice QCD: Isospin-1 KK scattering length*, *Phys. Rev. D* **96** (2017) 034510 [1703.04737].

[118] R. Brett, J. Bulava, J. Fallica, A. Hanlon, B. Hörz and C. Morningstar, *Determination of s- and p-wave $I = 1/2$ $K\pi$ scattering amplitudes in $N_f = 2+1$ lattice QCD*, *Nucl. Phys. B* **932** (2018) 29 [1802.03100].

[119] [ETM 18B] C. Helmes, C. Jost, B. Knippschild, B. Kostrzewa, L. Liu, F. Pittler et al., *Hadron-Hadron Interactions from $N_f = 2+1+1$ Lattice QCD: $I = 3/2$ πK Scattering Length*, *Phys. Rev. D* **98** (2018) 114511 [1809.08886].

[120] B. Moussallam, *N(f) dependence of the quark condensate from a chiral sum rule*, *Eur. Phys. J. C* **14** (2000) 111 [hep-ph/9909292].

[121] S. Descotes-Genon, L. Girlanda and J. Stern, *Paramagnetic effect of light quark loops on chiral symmetry breaking*, *JHEP* **01** (2000) 041 [hep-ph/9910537].

[122] [HPQCD 13A] R. Dowdall, C. Davies, G. Lepage and C. McNeile, *V_{us} from π and K decay constants in full lattice QCD with physical u, d, s and c quarks*, *Phys.Rev.* **D88** (2013) 074504 [1303.1670].